



This is to certify that the
thesis entitled
POWDER PROCESSING OF COMPOSITE PREPREG TAPE:
PARTICLE SIZE EFFECTS

presented by

SANJAY PADAKI

has been accepted towards fulfillment
of the requirements for

MS degree in CHEMICAL ENGINEERING

Handwritten signature of Lawrence T. Dyal in cursive script.

Major professor

Date MARCH 23, 1992

**LIBRARY
Michigan State
University**

**PLACE IN RETURN BOX to remove this checkout from your record.
TO AVOID FINES return on or before date due.**

<small>MAGIC 2</small> DATE DUE	DATE DUE	DATE DUE
JAN 14 1999 _____	_____	_____
_____	_____	_____
_____	_____	_____
_____	_____	_____
_____	_____	_____
_____	_____	_____
_____	_____	_____

**POWDER PROCESSING OF COMPOSITE PREPREG
TAPE : PARTICLE SIZE EFFECTS**

By

Sanjay Padaki

A THESIS

*Submitted to
Michigan State University
in partial fulfillment of the requirements
for the degree of*

MASTER OF SCIENCE

**Department of Chemical Engineering
Composite Materials and Structures Center**

1992

ABSTRACT

POWDER PROCESSING OF COMPOSITE PREPREG TAPE : PARTICLE SIZE EFFECTS

By

Sanjay Padaki

The effect of polymer powder particle size on the final volume fraction of the prepreg tape produced by the powder prepreg process and on the differences in its subsequent consolidation was the major focus of this investigation. As part of the study, process enhancements in the areas of aerosolizer wall caking and particle agglomeration were made. A semi-empirical model for the process of spreading the fiber tow was also developed.

The results indicate that an optimum polymer powder particle size range exists for the fabrication of prepreg tape with this fiber-matrix combination in this process. However, the effect of particle size on consolidation efficiency was not conclusive.

During this investigation, two new applications for the powder prepreg process were developed. A possible method for creating porous, formable RTM preforms from prepreg tape made from large particle sizes and low matrix volume fractions was developed. A second application demonstrated that hollow glass sphere filler material could be fluidized and deposited in a discontinuous, random fiber mat.

ACKNOWLEDGEMENTS

I would like to thank Dr. L. T. Drzal for his constant guidance and support throughout the course of this work.

This study is based on the investigation conducted by Dr. S. R. Iyer and I would like to acknowledge his work. I am also grateful to MMPI who financially supported this investigation.

I have taken the assistance of my colleagues on numerous occasions and I am indebted to them. In particular, I wish to thank Murty for his suggestions and assistance at various times.

Finally, I would like to thank my family who have been a constant source of support and encouragement.

TABLE OF CONTENTS

List of Tables	... vi
List of Figures	... vii
1. Introduction	... 1
2. The Process	... 7
2.1 Process Description	... 7
<i>2.1.1 Fiber spool</i>	... 9
<i>2.1.2 Spreader</i>	... 10
<i>2.1.3 Aerosolizer</i>	... 10
<i>2.1.4 Heater</i>	... 14
2.2 Process Automation	... 14
<i>2.2.1 Fiber motion</i>	... 16
<i>2.2.2 Oven temperature</i>	... 16
<i>2.2.3 Data acquisition</i>	... 17
2.3 Supplementary Process Description	... 17
<i>2.3.1 Volume fraction determination</i>	... 17
<i>2.3.2 Consolidation</i>	... 17
<i>2.3.3 Polishing and analysis</i>	... 18
3. Material Properties	... 21
3.1 Fiber Reinforcements	... 21
<i>3.1.1 Unidirectional carbon fiber</i>	... 21
<i>3.1.2 Glass fiber mat</i>	... 21
3.2 Matrix	... 24
3.3 Filler material	... 24

4. Process Enhancements	... 30
4.1 Line Speed Control	... 30
4.2 Caking of Aerosolizer Walls	... 32
4.3 Agglomeration	... 36
4.4 Particle Concentration Measurement	... 43
5. Process Modelling	... 45
5.1 Choice of Modelling Technique	... 45
5.2 Model Development	... 46
5. Particle Size Effects	... 54
5.1 Prepregging Experiments	... 55
5.2 Consolidation Experiments	... 60
6. New Applications	... 66
6.1 RTM Preform Manufacture	... 66
6.2 Impregnation of Fillers	... 70
8. Conclusions	... 77
Appendix	... 80
Bibliography	... 82

LIST OF TABLES

Table 1.1	Comparison of matrices
Table 1.2	Popular thermoplastic matrices
Table 2.1	Sample calculation of volume fraction
Table 3.1	Properties of polyamide and carbon fiber
Table 3.2	Properties of SCOTCHLITE™ glass bubbles
Table 4.1	Governing equations of particle interaction forces
Table 5.1	Parameters involved in spreader modelling
Table 5.2	Spreading experiments on AS4 carbon fiber at constant amplitude, varying frequency
Table 5.3	Spreading experiments on AS4 carbon fiber at constant frequency, varying amplitude
Table 6.1	Results of prepregging experiments
Table 7.1	Parameters and weights of typical impregnation run

LIST OF FIGURES

- Figure 2.1** Schematic of powder prepregging process
- Figure 2.2** Schematic of the spreader
- Figure 2.3** Schematic of the aerosolizer
- Figure 2.4** Schematic of the control loop
- Figure 2.5** Typical consolidation cycle
- Figure 3.1** SEM micrograph of Orgasol powder
- Figure 3.2** Particle size distributions of Orgasol powders
- Figure 3.3** DSC thermograms of as received Orgasol powder (A) 5 microns (B) 10 microns (C) 20 microns (D) 65 microns
- Figure 3.4** Variation of sintering time with temperature and particle size for polyamide
- Figure 3.5** Particle size distribution of SCOTCHLITE™ glass bubbles
- Figure 3.6** SEM micrograph of SCOTCHLITE™ glass bubbles
- Figure 4.1** Schematic of modified control strategy
- Figure 4.2** Schematic of buzzer mechanism
- Figure 4.3** Variation of sound pressure level with time
- Figure 4.4** Characterization of fluidized powders by Geldart
- Figure 4.5** Trend of charge to mass ratio with specific surface area
- Figure 4.6** Schematic of Real-time Aerosol Monitor
- Figure 5.1** Comparison of model and data of spread width versus frequency
- Figure 5.2** Comparison of model and data of spread width versus amplitude
- Figure 6.1** Variation of V_m with amplitude
- Figure 6.2** Schematic of consolidation mold
- Figure 6.3** Plot of consolidation pressure versus V_m
- Figure 7.1** Photograph of mold with preform
- Figure 7.2** SEM photograph of RTM preform
- Figure 7.3** Schematic of aerosolizer for filler impregnation

Figure 7.4 Frequency versus bed height at various amplitudes for 18" diameter aerosolizer (Amplitude values are relative)

Figure 7.5 SEM photograph of hollow glass sphere on glass fiber

Chapter 1

INTRODUCTION

Composite materials, as the name suggests, are a combination of two or more materials. These individual materials are physically and mechanically separate components, each having its own set of properties. In a composite they are combined to produce a composite material that has significantly better properties than either of its constituents alone.

Composite materials can be categorized into three groups :

- a) **Fibrous Composites** : consisting of either short, long or continuous fibers in a matrix.
- b) **Laminated Composites** : consisting of layers of different materials.
- c) **Particulate Composites** : consisting of particles of one or more materials enveloped in a matrix.

Fibrous composites will be the main focus of this dissertation. Popular fibers in use currently are carbon, glass and aramid. The matrix material used with these fibers varies with the application. They can be ceramics, metals or polymers. Polymer matrix composites are used in the majority of today's aircraft, automotive, sporting goods and other related industries. Polymer matrices are of two types - thermoset and thermoplastic. Thermoset matrices such as epoxy resins are used in the majority of composite applications because of their ease in processing, low shrinkage, good adhesion and

excellent chemical resistance. The drawbacks of using thermoset resins are their limited shelf life (coupled with expensive storage costs), low resin strengths and brittleness. Thermoplastic matrices offer potential for lower cost manufacturing due to their indefinite prepreg stability, fast processing cycles, ease in storage, ability to be reprocessed, high fracture toughness, good damage tolerance and impact resistance, good resistance to micro-cracking and ease in quality control. They also have their own drawbacks such as difficulty in processing because of inherently high viscosity, solvent sensitivity and poor quality of the prepreg tape. Table 1.1 compares the properties of thermoset and thermoplastic matrices for composites. Table 1.2 lists the popular thermoplastic matrices in use today along with their T_g 's and T_m 's.

The T_g or glass transition temperature of a polymer is the temperature below which the polymer molecule is frozen in position and exists in a glassy state. At this stage all molecular motion of the polymer chains ceases. The T_g is affected by a number of factors including polydispersity and rate of cooling. The melting temperature, T_m , of a polymer is the temperature at which there is an abrupt change in volume and coefficient of thermal expansion of the material. Both T_g and T_m are practically important. T_g sets an upper temperature limit for use of amorphous thermoplastics like polystyrene and a lower temperature limit for rubbery behavior of an elastomer like SBR rubber. With semicrystalline thermoplastics, T_m or the onset of the melting range determines the upper service temperature. Between T_m and T_g , semicrystalline polymers tend to be rough and leathery. Brittleness of the amorphous regions begins to set in below T_g . As a general rule the working temperature range for semicrystalline plastics is between T_g and a practical softening temperature which lies above T_g and below T_m [1]. However, the viscosity of thermoplastics in this working temperature range is still extremely high and is one of the main problems facing the processing of thermoplastic composites.

Table 1.1 Comparison of matrices ^[2]

Property	Thermoset	Thermoplastic
Weight	+	+
Material Cost	+	+
Processing cost-reduction potential		+
Simplicity of chemistry		+
Melt flow	+	
Prepreg tack and drape	+	
Long prepreg shelf life		+
Low processing temperature	+	
Low processing pressure	+	
Low processing cycle time		+
Low cure shrinkage		+
Quality control data base	+	
Mechanical property data base	+	
Ability to translate fiber properties	+	+
Solvent resistance	+	
Corrosion resistance	+	+
Resilience	+	
Toughness		+
Lack of time-dependance	+	
Interfacial adhesion	+	
Low thermal expansion	+	

Table 1.2 Popular thermoplastic matrices

Name	T_g °C	T_m °C
Victrex PEEK <i>poly ether ether ketone</i>	143	343
BASF Ultrapek <i>poly ether ketone ether ketone ketone</i>	175	375
DuPont PEKK <i>poly ether ketone ketone</i>	156	338
Ryton PPS <i>poly phenylene sulfide</i>	90	285
LaRC-TPI <i>thermoplastic imide</i>	217-229	275-305
Radel C <i>poly ketone</i>	260	none
Torlon C <i>poly amide imide</i>	275	none

Many solutions have been presented to the problem of processing thermoplastic composites. These include:

- ★ *Co-mingling* - weaving reinforcing fibers with thermoplastic matrix fibers together to get a shapeable fabric.
- ★ *Filament bundle coating* - sheathing small filament bundles with the thermoplastic polymer.
- ★ *Film stacking* - compacting alternate layers of fiber with thin sheets of resin.
- ★ *In-situ polymerization* - preimpregnating the fiber tow with a low molecular weight prepolymer and subsequently polymerizing a linear chain in situ.
- ★ *Melt impregnation* - forcing molten polymer into a fiber tow to form a prepreg tape.

- ★ *Powder prepegging* - impregnating the fiber tow with a dry powder form of the polymer.
- ★ *Slurry processing* - Drawing the fiber tow through a suspension of solid, small polymer particles suspended in a liquid carrier.
- ★ *Solution processing* - dissolving the resin in a suitable solvent and impregnating the tow with dilute solution which is later processed to remove solvent.

The final product of all the above processes (i.e. a material containing the reinforcing fibers and polymer in an unconsolidated form) is called a prepreg. Prepreg can be in the form of tape, laminates or fabric. These can be converted into useful parts and components by a variety of processes usually involving the application of heat and pressure.

In the case of thermoset polymer composites the prepreg is in a partially reacted state called a B-staged part. This is because the part is not completely cured. The B-staged part needs to be kept under refrigerated conditions in order to prevent unwanted curing. In order to get an "useful" part, the polymer chemical reaction needs to occur in the composite which completes the cross-linking of all of the polymer chains. This reaction often takes several hours of staged heat treatment. Once the reaction is completed, the part cannot be processed again.

Thermoplastic polymer composite materials do not need to undergo a reaction. They are molded by simply applying heat and pressure to a geometrical arrangement of prepreg. This results in faster processing times. Due to the absence of chemical reactions, thermoplastics have an indefinite shelf life thus reducing handling costs. In

order to get a final part the layers or plies of prepreg tape are laid up in the desired configuration. Any one of the processing methods of stamp molding, laminating, diaphragm forming, thermoforming, pultrusion, or filament winding can then be used to get the final composite part.

Thus thermoplastic composites offer a number of potential advantages over the traditional thermoset matrix composites but the inherent difficulty in their processing has required newer processing technologies to be developed. One of them based on a polymer powder prepregging strategy has been developed here at Michigan State University [3]. The emphasis of the present work was to investigate particle size effects on the performance of the process and explore new applications for it.

Chapter 2

THE PROCESS

The powder prepegging process has many advantages over the other processes listed in Chapter 1. The following are the most important features of the process :

- a) The average particle size used is approximately in the same order as the dimensions of the fiber. This enables a precise control over volume fraction. This also removes matrix viscosity as a variable in the process since the polymer melt has to flow only over small distances.
- b) Spreading of the fibers enables almost every fiber to be completely wetted by the matrix.
- c) The deposition of the matrix onto the fiber can be controlled precisely and over a wide range of volume fractions.
- d) The prepreg tape obtained from the process has good tack and drape qualities.
- e) The tape can be easily laid up and transformed into a composite part by using simple consolidation cycles.

This chapter describes the various components of the powder prepreg process [4], the subsequent steps to get a final part and the analysis of the part.

2.1 Process Description

Figure 2.1 shows a schematic of the entire system. A tow of continuous fiber is unwound from the fiber spool (E) by the nip rollers through a guide slot (I). The nip

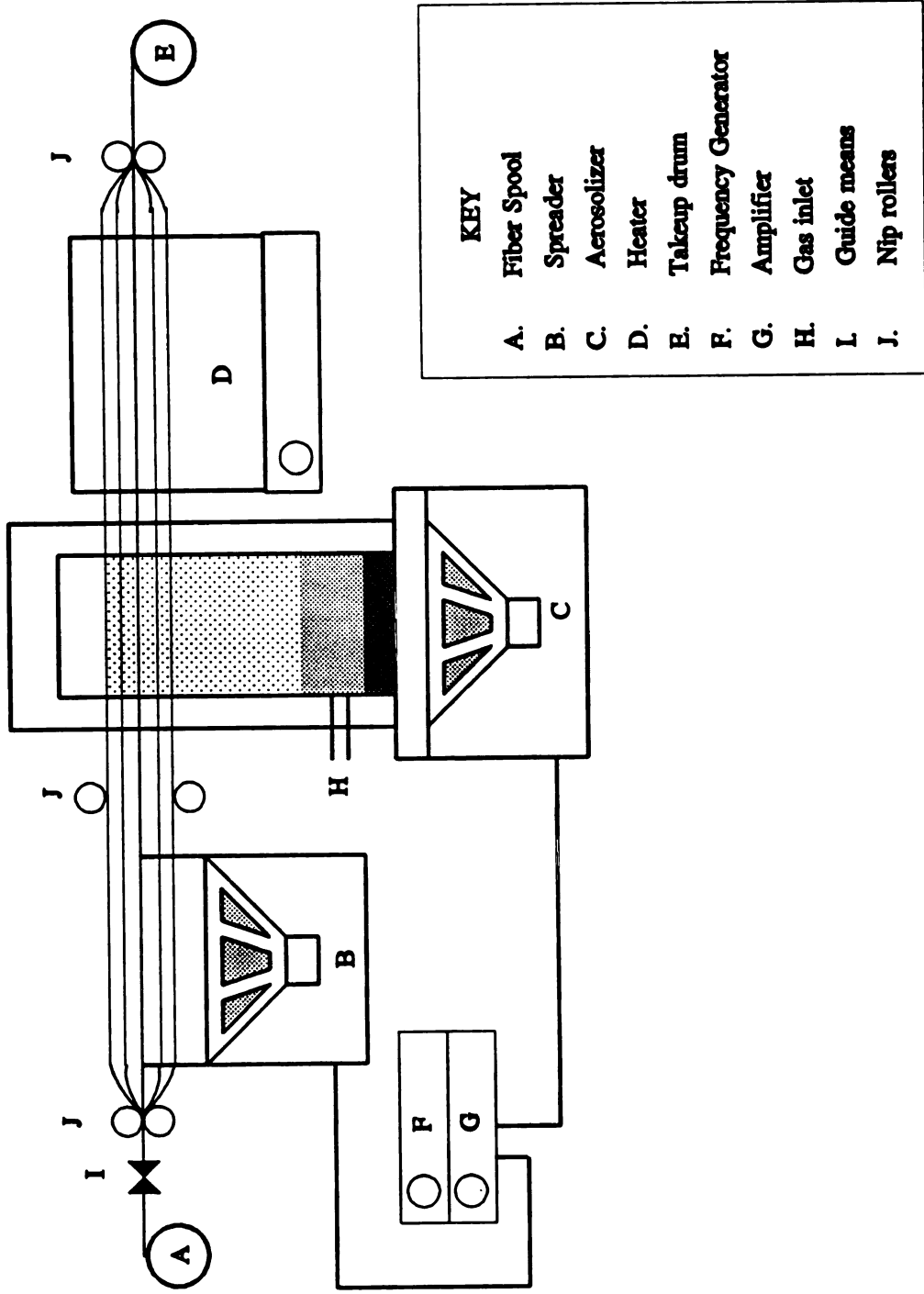


Figure 2.1 Schematic of powder prepegging process

rollers (J) are all motor driven. The tow passes over the spreader (B) where it is separated into individual filaments. The section of the tow after passing through the spreader remains separated though this may not be obvious from the diagram. The spread tow enters a particle deposition chamber called the aerosolizer (C) where it picks up the polymer powder. The particle deposition is via an aerosol. The generation of the aerosol is achieved through an acoustic vibration process which will be explained later in this chapter. Dry nitrogen is supplied into the aerosolizer through the inlet (H). The particles deposited on the fibers in the aerosolizer are sintered in the heater (D). The frequency generator (F) and amplifier (G) provide the acoustic energy to the spreader and aerosolizer. The prepreg tape produced by the process is wound onto the take-up drum (E).

2.1.1 Fiber spool :

The fiber spools are basically fiber unwinding and winding mechanisms. Continuous fiber is commercially produced in rolls which are either internally or externally wound and can be directly fitted to the unwinding spool. There is no motor drive on this spool and the unwinding of the fiber tow is achieved by the tension supplied to the tow through the nip rollers.

The take-up spool serves to wind the prepreg tow produced by the process and is driven by a variable speed motor. The motor speed is matched to the speed of the process by adjusting the voltage supplied to it. The entire take-up drum setup is mounted on a movable stage. The stage is driven by a linear motor and thus moves the spool in lateral directions. A combination of the rotary and transverse motion causes the prepreg tape to raster across the entire spool to maintain an uniform layer. Limit switches at the

ends of the motion reverse the direction of lateral travel when the tape reaches the end of the spool.

2.1.2 Spreader :

The spreader is a patented device which operates using acoustic energy [5]. The basic function of the device is to spread the incoming fiber tow into a plane so that individual fiber filaments are exposed. This is necessary for the downstream section of the process when each individual filament needs to be coated with matrix. A diagram of the spreader is shown in Figure 2.2.

The spreader is made up of a speaker over which a number of highly polished stainless steel rods are mounted. The fiber tow is threaded through these rods. These rods are mounted on frictionless bearings and rotate when there is tension in the tow. The underlying principle is that when fibers are vibrated the individual filaments are shaken apart from the bundles of fiber present in the tow. The rods serve as nodes for the vibrating fiber filaments. The speaker placed below the rods provides the acoustic energy. A function generator coupled with an amplifier provide the energy source for the speaker. Normal operation of the system requires acoustic energy at around 35 hz and 12 V which gives the maximum spreading widths. In order for efficient spreading the tension in the spreader should be zero. This is achieved by placing nip rollers at the ends of the spreader. The two rollers are coupled mechanically and so exert no tension on the tow between them.

2.1.3 Aerosolizer :

The aerosolizer is also a patented device and is the key component in the system [6]. The purpose of the aerosolizer is to generate a controlled concentration of an

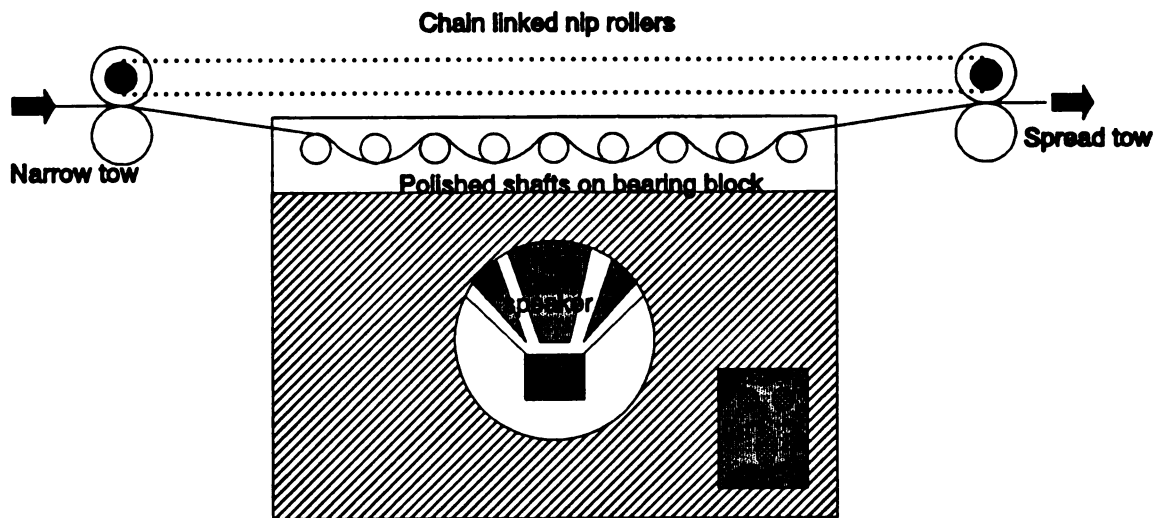


Figure 2.2 Schematic of the spreader

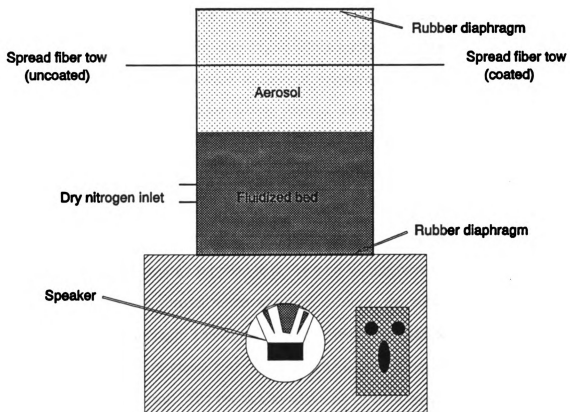


Figure 2.3 Schematic of the aerosolizer

aerosol of fine polymer particles that then adhere to the individual filaments in the spread fiber tow. Figure 2.3 shows the basic parts of the aerosolizer.

The spread tow that emerges from the spreader enters and exits the aerosolizer through two coplanar slots made in the acrylic tubing which forms the body of the aerosolizer. The aerosolizer operates in a batch mode with the polymer powder being charged into the chamber at the beginning of the run. The top and bottom of the chamber are closed off by rubber diaphragms which are held in place by O-rings. A dry nitrogen gas inlet serves to provide an inert atmosphere and a constant buoyant force within the chamber. The speaker which vibrates the air column inside the chamber draws its power from a 100 watt amplifier which is coupled to a sine wave generator.

The main process behind the operation of the aerosolizer is the generation of the aerosol. The bed at the bottom of the aerosolization chamber serves as a reservoir for powder particles. The energy supplied to the speaker is transferred to the bed and to the air column within the aerosolization chamber through the rubber diaphragm. The oscillation of the diaphragm causes the bed of powder to fluidize. The fluidization results in the collision of clusters of powder particles which releases a fine stream of powder termed the aerosol. The oscillation of the air column coupled with the buoyant force of the nitrogen stream carries the aerosol to the top of the chamber where it interacts with the spread fiber tow. This entire process is termed aerosolization.

Normal operating conditions require resonance in the column which is gaged by visual observation of the diaphragms. At resonance the diaphragms oscillate with maximum amplitude. The voltage supplied to the system determines the maximum

amplitude and the average volume fraction of the outgoing tow. This can range from 6 to 12 volts (rms) with corresponding V_f (fiber) ranging from approximately 90% to 50%. A sound level meter placed at the height of the fiber tow monitors the sound pressure level in decibels within the system.

2.1.4 Heater :

The purpose of the heater is to sinter the polymer particles to the fiber tow. The tow from the aerosolizer has particles adhering to it only by molecular and electrostatic forces. To prevent loss of matrix during subsequent handling, these particles must sinter, coalesce and adhere to the tow. The heater is a normal convection type oven (VWR 1300, 750 Watts) and is capable of achieving temperatures up to 250 °C. The oven has been modified for the process by machining slits in the front and back. The top half of the oven has been sealed off with insulation in order to provide a more concentrated heat source.

2.2 Process Automation

The different components of the system described in Section 2.1 are integrated into a control system. A schematic of the control system is shown in Figure 2.4. The control software is run by a Hewlett-Packard personal computer QS/16S with an interface card (Data Translation DT2811-PGH), a controller box (Composite Line Controller or CLC) and various sensors monitoring the process. Three main tasks are performed by the control system :

- a) Fiber motion control
- b) Oven temperature control
- c) Data logging of process variables

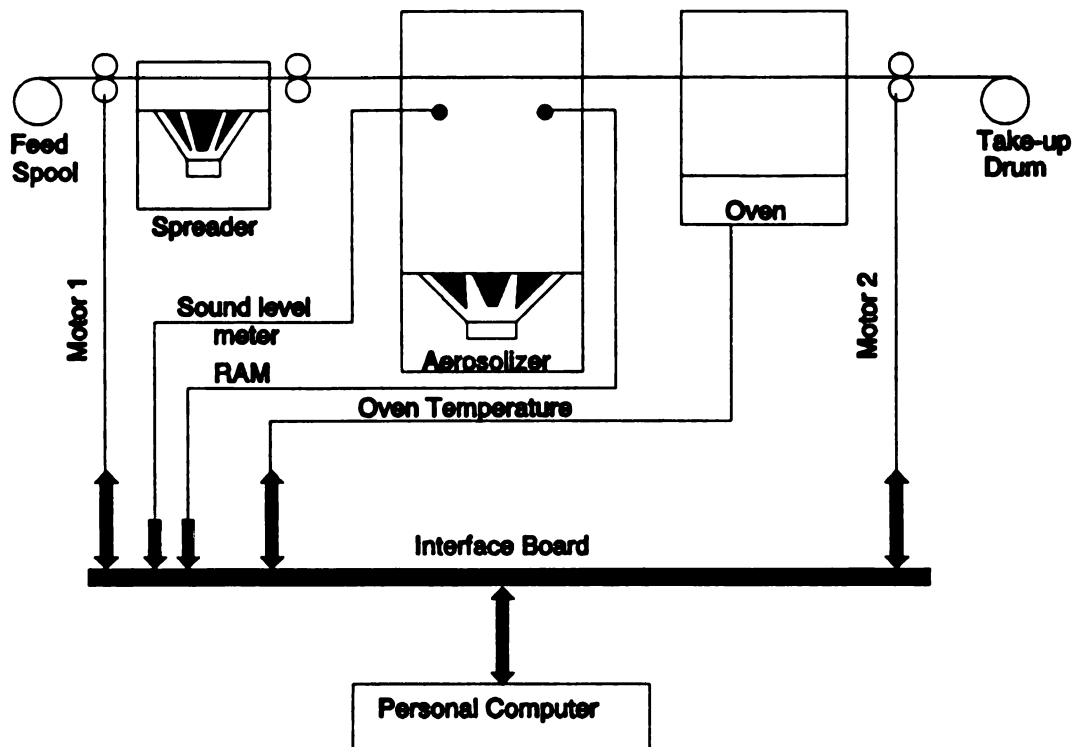


Figure 2.4 Schematic of the control loop

2.2.1 Fiber motion :

The fiber motion system is a critical part of the powder prepreg process. Variations in the tow speed result in uneven particle pick-up leading to variations in the volume fraction of the prepreg tape. Fluctuations in the tow speed could also lead to tow breakage or tow scatter. A feedback controller is used in order to maintain a constant line speed. The controller operates the two nip roller motors as shown in Figure 2.4. The feedback control is a C language software program that is run on a personal computer. The equation governing the PID control loop is [7]

$$P_n = \bar{p} + K_c \left[e_n + \frac{\Delta t}{2\tau_I} (e_k + \frac{e_{k-1}}{2}) + \frac{\tau_D}{\Delta t} (e_n - e_{n-1}) \right] \quad (1)$$

Both motors operate on a 10 V d.c. power supply and are controlled by similar PID loops. The values of the constants K_c , τ_D and τ_I for the two motors are input to the control program. The take-up drum is driven by its own d.c. motor and runs at a constant base speed. The direction of travel of the lateral motion motor is switched through the program by sensing the output from the limit switches.

2.2.2 Oven temperature :

The oven temperature needs to be controlled in order to get the proper quality of prepreg tape. High temperatures lead to stiff prepreg tapes while low temperatures do not sinter the particles to the fiber. The temperature is controlled by the control program through an on-off control loop. The temperature in the oven is sensed by a K-type thermocouple. The voltage signal is converted into a digital signal by an interface card. The output of the feedback loop is sent to a switching unit that switches the oven on or off depending on the deviation from the set point. The set point itself is an input to the control program.

2.2.3 Data acquisition :

The control program logs data from the process during the run. The variables that are logged are time, motor speeds along with standard deviations, temperature and sound level. In addition the particle concentration signal from the Real Time Aerosol (RAM) monitor is also logged.

2.3 Supplementary Process Description

In order to fully study the effects of a particular variable on the process, a number of subsequent experiments must be carried out to characterize the prepreg tape that is manufactured and are described below.

2.3.1 Volume fraction determination :

Prepreg tape made from the process is cut into known lengths. A number of them (typically three out of every ten lengths) are weighed in order to get a statistical distribution of weights over the run. Knowing the average weight of a similar length of bare fiber, an approximate average value for the fiber weight fraction (W_m) is determined. Using the appropriate densities for fiber and matrix a fiber volume fraction (V_f) is calculated. The matrix volume fraction (V_m) can then be calculated by subtracting from 1.0. A sample calculation is shown in Table 2.1.

2.3.2 Consolidation :

In order that a final part be made, it is necessary to consolidate the prepreg tape obtained from running the prepregging process. The prepreg tape is cut up and laid up in a matched die chrome steel mold. Non-porous Teflon[®] film is placed between the mold surfaces and the lay-up to facilitate easy removal of the part after consolidation. A requisite amount of pressure and temperature is applied in a simple consolidation cycle

Table 2.1 Sample calculation of volume fraction

Sample length, inch	=	32
Weight of 32" of prepreg tape, gm	=	W_{32}
Weight/cm of prepreg tape, gm/cm	=	$W_{32} / (32 \times 2.54)$
	=	W_1
Weight/cm of bare fiber, gm/cm	=	W_2
Weight/cm of matrix, gm/cm	=	$W_1 - W_2$
	=	W_3
Weight fraction fiber	=	W_2 / W_1
	=	W_f
Density of fiber, gm/cc	=	δ_f
Density of matrix, gm/cc	=	δ_m
Volume/cm fiber, cc/cm	=	W_2 / δ_f
	=	V_1
Volume/cm matrix, cc/cm	=	W_3 / δ_m
	=	V_2
Volume fraction (fiber)	=	$V_1 / (V_1 + V_2)$
	=	V_f

as shown in Figure 2.5. The equipment used for the process is a plate and frame press (Carver press) with both heating and cooling capabilities. The temperature in the mold is detected by a K-type thermocouple placed within the mold face. Consolidation pressure is calculated based on the load applied on the area of the lay-up rather than on the area of the mold.

2.3.3 *Polishing and analysis :*

In order to view the sample under the microscope to determine V_f and V_v , it is necessary to polish the surface of the composite to below 0.05 micron grit. A section from the consolidated part is cut using a diamond saw and mounted in an acrylic holder. The direction of mounting ensures a cross-sectional view of the sample. The sample is polished in successive steps using a 80 grit belt sander, Struers Abramin Automated Polisher (240,320,1000,2400 and 4000 grit), LECO GP20 Grinder/Polisher (5 micron and 1 micron) and a Buelher Vibromet (0.05 micron). The polished samples are cleaned

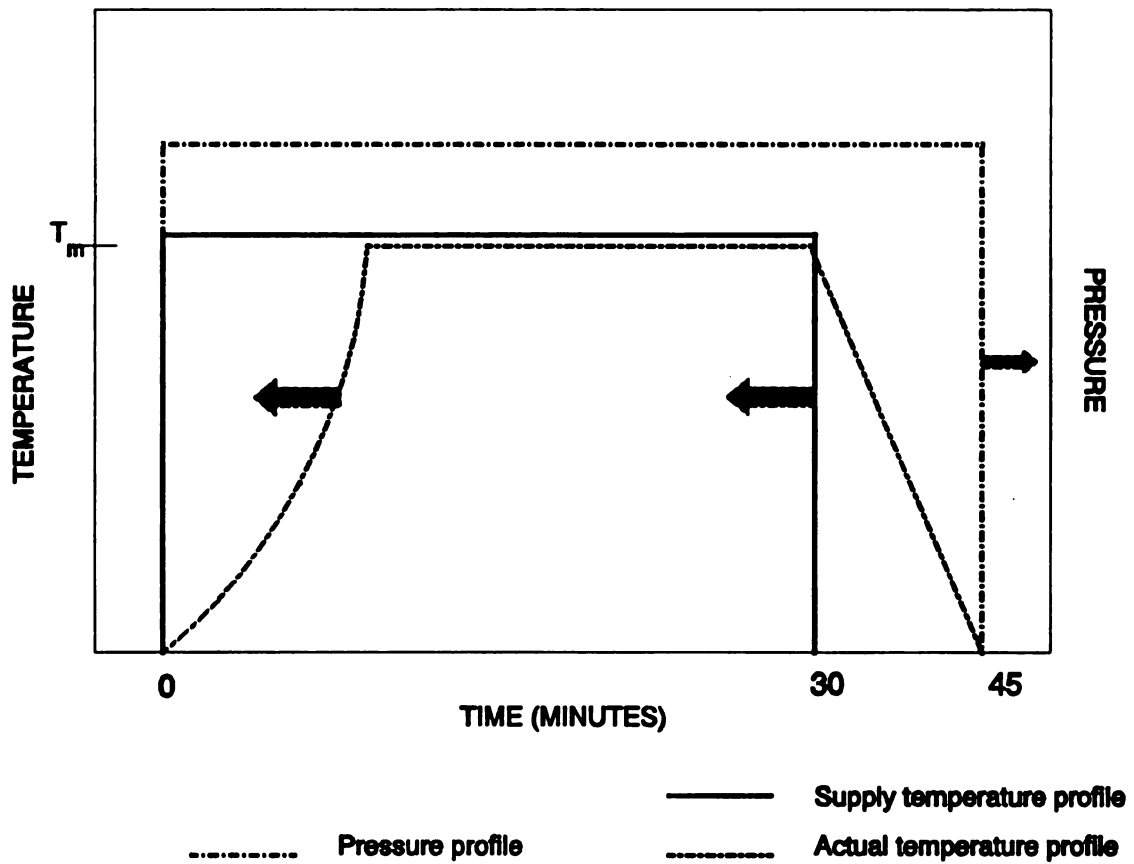


Figure 2.5 Typical consolidation cycle

in an ultrasonic bath and then with ethanol. An Olympus microscope with a video camera attachment is used along with a Amiga personal computer in order to digitize 15 random images. The digitized images are then analyzed for volume fraction and void fraction using the ONVFA (Optical Numeric Volume Fraction Analysis) program [8]. The program counts the number of fibers in a given screen and calculates the fraction occupied by them. Void fraction analysis is a little subjective since the grey levels from a histogram are used in the determination.

In summary, various parameters in the process need to be analyzed and the sequence of prepregging, consolidation, mounting, polishing and volume fraction analysis needs to be performed for each set of these parameters. This would give an understanding of the effects of operating variables on the powder prepreg process and help in scale-up and commercial application of the process.

Chapter 3

MATERIAL PROPERTIES

The materials used in the investigation of particle size effects were carbon fiber reinforcement and polyamide matrix. A new application based on hollow glass spheres and random glass fiber mat was also investigated in the present study. This chapter discusses the properties of these components.

3.1 Fiber Reinforcements

3.1.1 Unidirectional carbon fiber :

The reinforcing fiber used was the PAN (polyacrylonitrile) based unsized Hercules AS4-3K carbon fiber consisting of 3000 fibers per tow. The mean diameter of the fibers is 8.0 microns.

3.1.2 Glass fiber mat :

Two types of random glass fiber mats manufactured by CertainTeed Corporation and designated as 816 and 850 were used. Each type has different weight percentages of a proprietary thermoplastic binder. The fiber mat is commercially supplied in 50" wide rolls. For the purposes of experimentation 12" x 12" sections were cut out from these rolls.

3.2 Matrix

The polyamide (Nylon-12) matrix material for this investigation was obtained from Atochem Inc. in the form of powders (commercial name Orgasol). Four different size ranges (mean sizes 5, 10, 20 and 65 microns) of the powder were obtained. The properties of all four powders are identical. Figure 3.1 is an SEM micrograph at 720X of the 10 micron Orgasol powder. Figure 3.2 shows the particle size distributions for the four powders. It can be noticed that the size distributions for the 5 and 10 micron powders are extremely tight while those for the 20 and 65 micron are much broader. Figures 3.3 (A,B,C,D) show DSC (Differential Scanning Calorimetry) thermograms for the four powders [9]. The thermograms indicate that the powders are very similar and their melting range is between 160 and 180°C. Figure 3.4 shows the variation of sintering time with temperature as the particle size is varied. This was estimated using Frenkel's theory [10] and the viscosity model for polyamide that was developed by Iyer [11]. A listing of the computer program and the program logic is attached in the Appendix.

3.3 Filler Material

A hollow glass sphere filler material was investigated. The filler is manufactured by 3M and is commercially called SCOTCHLITE™ Glass Bubbles. The glass bubbles combine low density with a high level of durability and chemical resistance. The size distribution of the filler is shown in Figure 3.5. Figure 3.6 is an SEM micrograph of the spheres at 200X.

The properties of the above materials are summarized in Tables 3.1 and 3.2.*.

* From manufacturer's literature

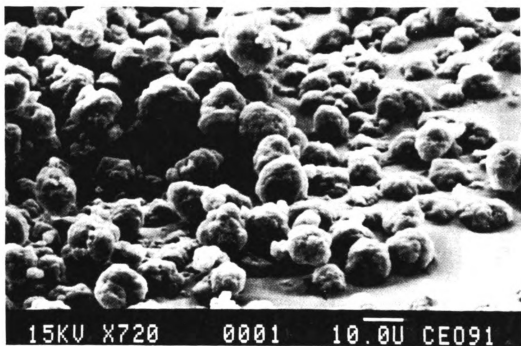


Figure 3.1 SEM micrograph of Orgasol powder

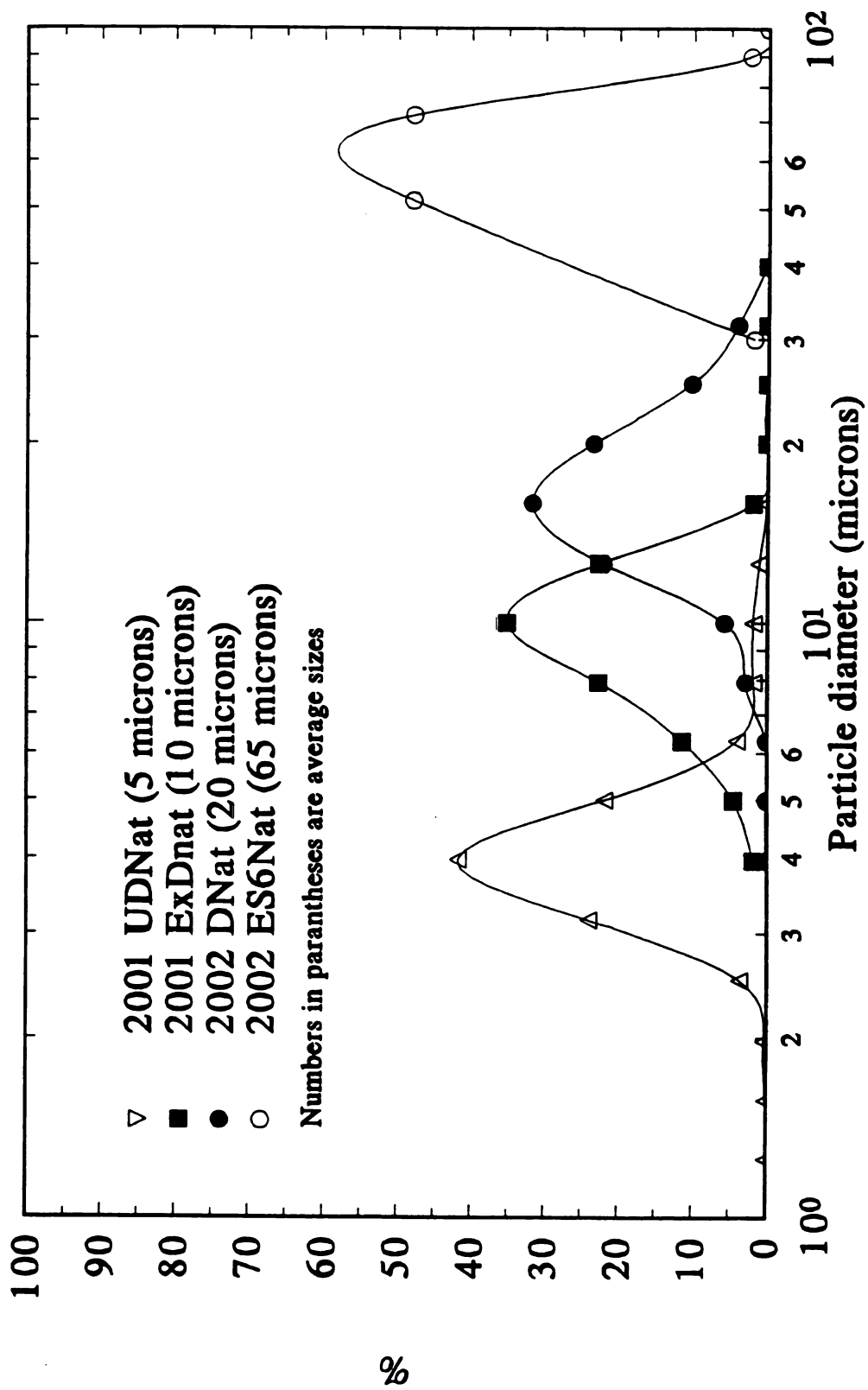


Figure 3.2 Particle size distributions of Orgasol powders

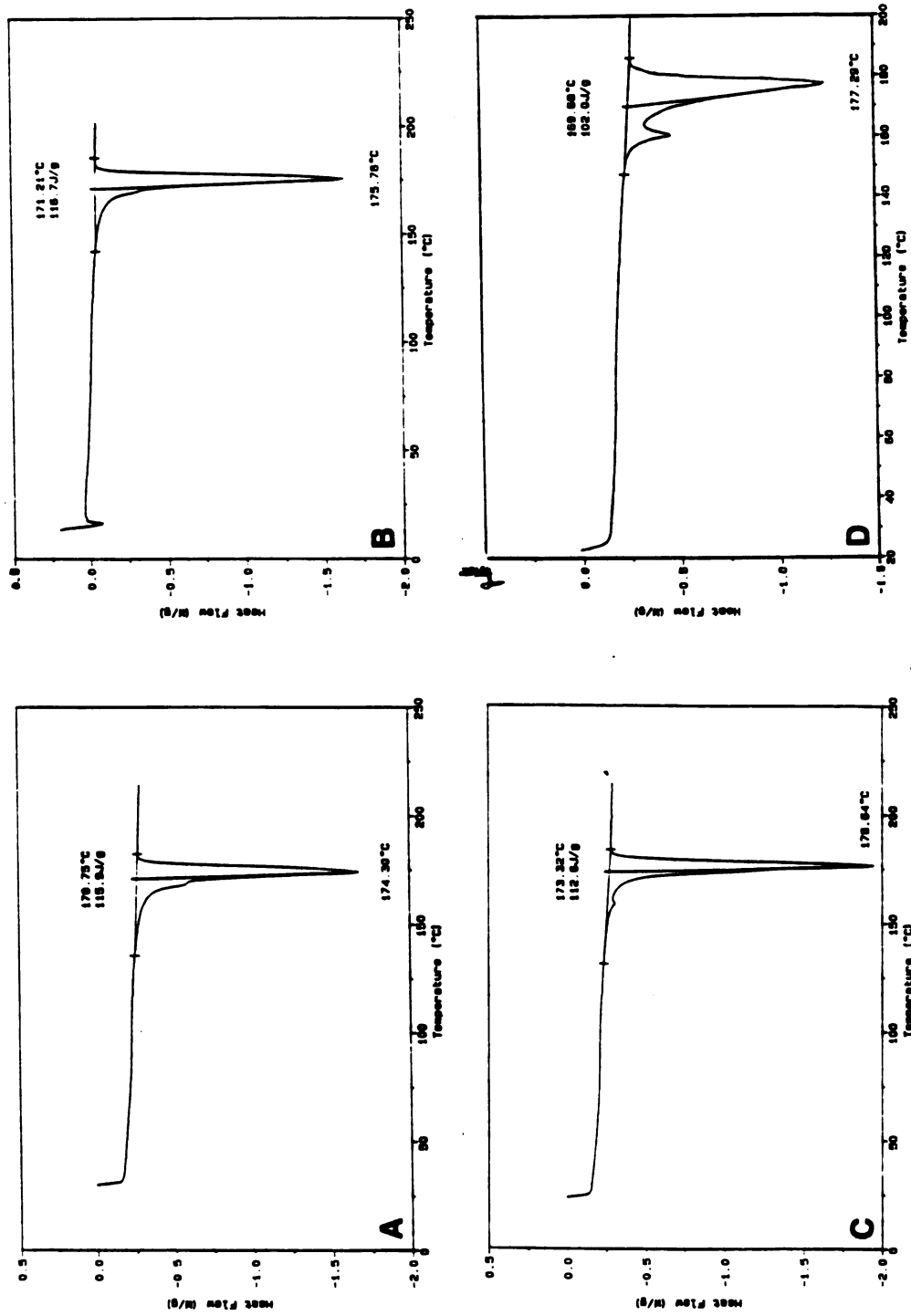


Figure 3.3 DSC thermograms of as received Orgasol powder (A) 5 microns (B) 10 microns (C) 20 microns (D) 65 microns

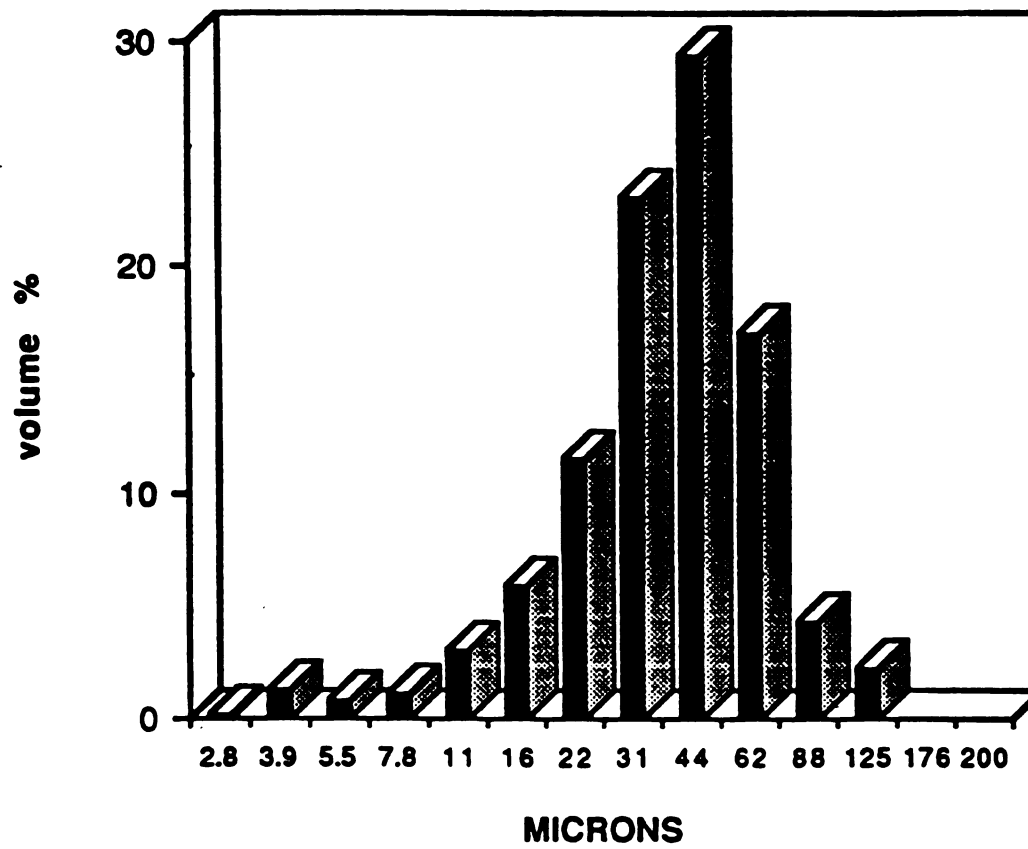


Figure 3.5 Particle size distribution of SCOTCHLITE™ glass bubbles

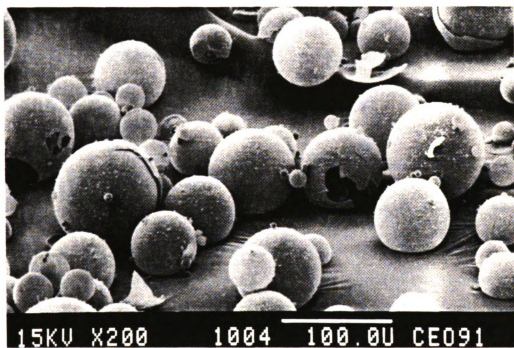


Figure 3.6 SEM micrograph of SCOTCHLITE™ glass bubbles

Table 3.1 Properties of polyamide and carbon fiber ^[12]

ORGASOL POLYAMIDE	
Specific gravity	1.02
Melt Temperature, °C	175
Specific heat, cal/gm/°C	
@ 40 °C	0.58
@ 140 °C	0.81
Thermal Conductivity, W/m/°C	0.22-0.31
Viscosity, Pa.s (0.1 sec ⁻¹ , 197.3 °C)	52.6
Surface tension, mJ/m ²	30.0
HERCULES AS-4 CARBON FIBER	
Diameter, microns	8.0
Specific gravity	1.80
Specific heat, cal/gm/°C	
@ 75 °C	0.22
@ 175 °C	0.27
Thermal Conductivity, W/m/°C	5.73

Table 3.2 Properties of SCOTCHLITE™ glass bubbles

Average particle density, g/cc	
Nominal	0.22
Range	0.19-0.25
Bulk density (range), g/cc	0.09-0.17
Floaters	
(% by bulk volume)	90
Thermal conductivity,	
BTU/hr/ft ² /°F/in @room temp.	0.2-1.2
Softening point, °C	715

Chapter 4

PROCESS ENHANCEMENTS

The process that has been described in the previous chapter has many shortcomings. One of the aims of this investigation was to refine certain sections of the process primarily to improve the control over volume fraction of the prepreg tape and also to aid in the development of a scaled-up version of the process. The chief problems with the present prepreg process are described below. Methods employed to overcome these difficulties are also described.

4.1 Line Speed Control

One of the drawbacks of the prepreg system is the line speed control strategy. The control method employed is the matching of speeds of the two separate fiber spool motors that are placed at the ends of the process. Exact speed monitoring is not possible by this technique due to the physical limitation of the control system. The speed of motor 1 is always fractionally different from that of motor 2. This difference in the speeds causes the fiber tow tends to scatter (when there is little tension) or break (when there is high tension). The uneven tension in the tow also results in variable tow spread width.

The possible solution to this problem is the employment of a new control strategy. A schematic of this strategy is shown in Figure 4.1. This strategy would involve

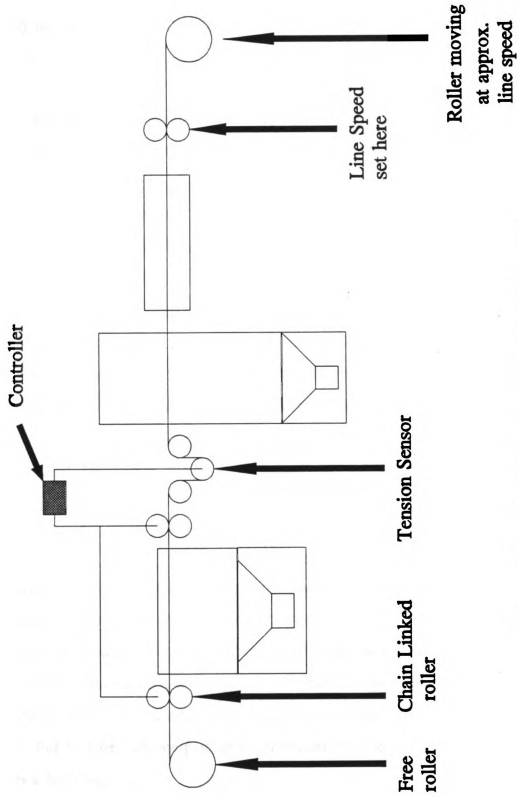


Figure 4.1 Schematic of modified control strategy

adjusting speed according to the tension in the tow. The tow speed itself would be set at only one point thus eliminating the problem of matching speeds of two independent motor drives.

4.2 Caking of Aerosolizer Walls

The caking of the walls of the aerosolizer by the polymer powder causes a drop in the volume fraction of the prepreg tape. The caking affects the system in two ways. First, it depletes the amount of powder available for aerosolization. Second, it changes the sound characteristics of the aerosolization chamber which in turn results in poor aerosolization. Both result in uneven powder deposition and variation in the volume fraction of prepreg tape.

Caking is a result of the high surface charges present on polymer particles. In order to quantify this surface charge, a simple equation listed below can be used.

$$\sigma = \frac{Q}{4\pi R^2}$$

where

σ = surface charge density

Q = total charge

R = radius of the particle

(2)

This equation indicates that as the radius of the particle decreases the charge density increases. It also indicates that as the total charge increases the surface charge increases. However, for a particle in air the surface charge density at the interface with air cannot grow to an infinitely high level due to the dielectric nature of air. Under normal conditions, the maximum value of the surface charge density is limited to 2.7×10^{-5} C/m². For a single 5 micron particle this translates into a total charge of 2.12×10^{-15} C and is a fairly high value.

In addition to the dielectric properties of air and the high charge density on the surface of the polymer particle, the particles themselves being insulators have very low dielectric constants. This causes the charges to concentrate on the surface without being dissipated into the surrounding medium. When a surface having dielectric constants lower than air is brought in the vicinity of the polymer powder, the particles tend to preferentially attach themselves to it and thus causes caking. In order to solve this problem, the charge must either be neutralized or a force greater than that exerted by the charge must be used on the powder particles to dislodge them.

Many techniques employing the above approaches were tried. The wall was coated with an antistick coating (fluro glide[®] CP, manufactured by Chemplast Inc.) but did not reduce the caking. An aluminum foil layer inside the chamber reduced the caking to a great extent. However, points of higher surface energy (e.g. fingerprints, surface roughness, etc.) acted as nucleation sites for wall caking. A silver coating on the inside of the chamber was also tried in order to reduce surface irregularities but did not show any additional improvement. A combination of surface charge dissipation and wall tapping was however extremely successful.

The wall tapping mechanism was a simple electromagnetic doorbell (buzzer). A schematic of the set-up is shown in Figure 4.2. The bell itself has been removed so that the arm of the buzzer raps against the side of the aerosolizer chamber. The frequency and time of rapping is controlled through a separate relay. The repeated rapping dislodges the accumulated particles from the wall. The effectiveness of the buzzer can be seen in Figure 4.3. The two runs have been performed at different amplitudes accounting for the fact that the average sound pressure levels (SPL) are different. However, the trend shows that there is a decrease in SPL when the buzzer is off. There

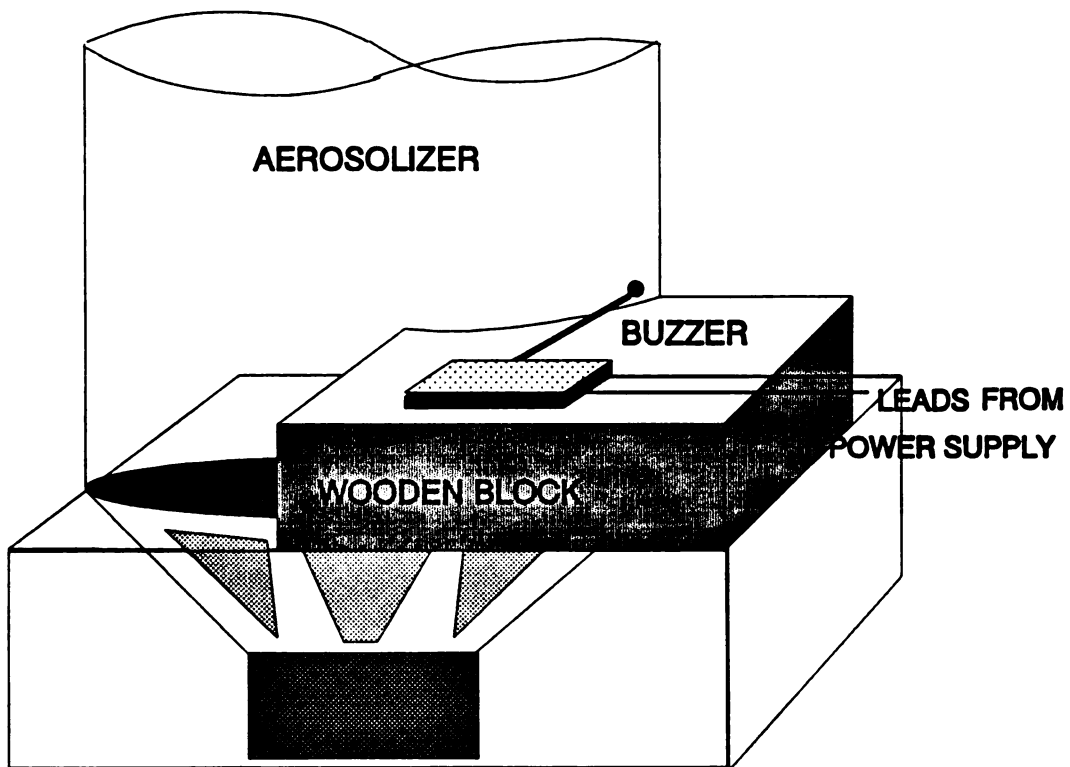


Figure 4.2 Schematic of buzzer mechanism

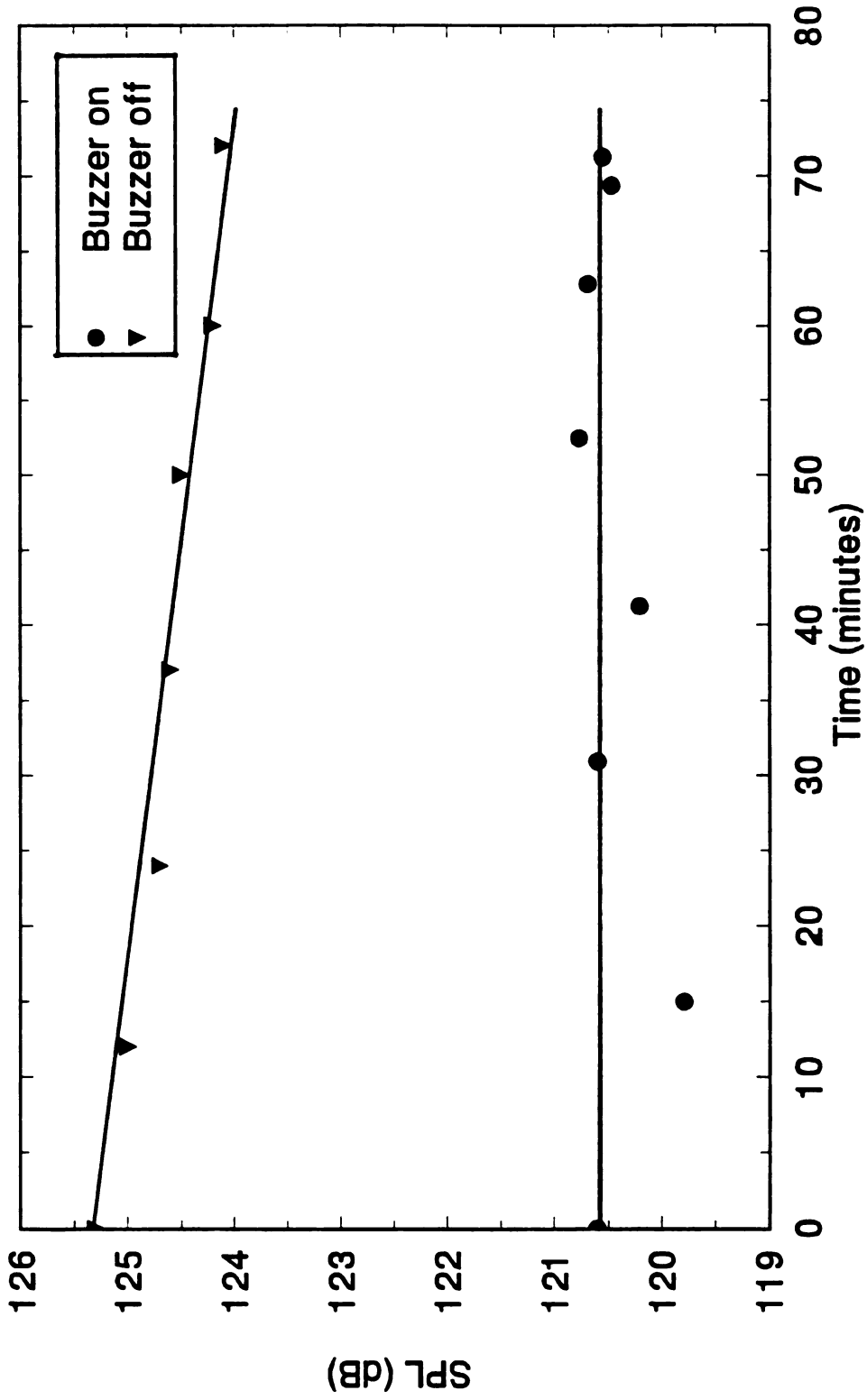


Figure 4.3 Variation of sound pressure level with time

is a scattering of SPL when the buzzer is switched on but the average SPL is almost constant throughout the run.

4.3 Agglomeration

Agglomeration of powder particles is a serious problem affecting the process. It results in poor particle pick-up and large fluctuations in the prepreg tape volume fraction during the run. In order to solve this problem a thorough understanding of the factors involved in the agglomeration process is necessary.

The high charge to mass ratio of smaller size polymer particles causes agglomeration when they are vibrated in the aerosolizer. Physically, agglomeration can be described as the association of a number of smaller particles forming a much larger particle. The degree of agglomeration depends on the charge to mass ratio of the individual particles. Reist [13] has proposed that particle agglomeration can occur in ordered flow such as that which can be established in a sonic field. Here agglomeration takes place by the different velocities imparted to particles of differing inertia, by aerodynamic attractive forces between the particles and by radiation pressure which moves the particle towards the vibration antinodes. In the aerosolizer a similar situation arises which causes the polymer particles to agglomerate.

However, agglomeration is not an universal phenomena. Only certain categories of powders tend to be cohesive in nature. Geldart [14] has classified all powders into four categories - Types A, B, C and D. Figure 4.4 shows the classification graphically. Type A powders are characterized by the fact that, when fluidized at a gas rate not too far above U_{mf} (the minimum fluidization velocity), the expansion is homogeneously distributed over the powder bed. When the gas rate is further increased above another

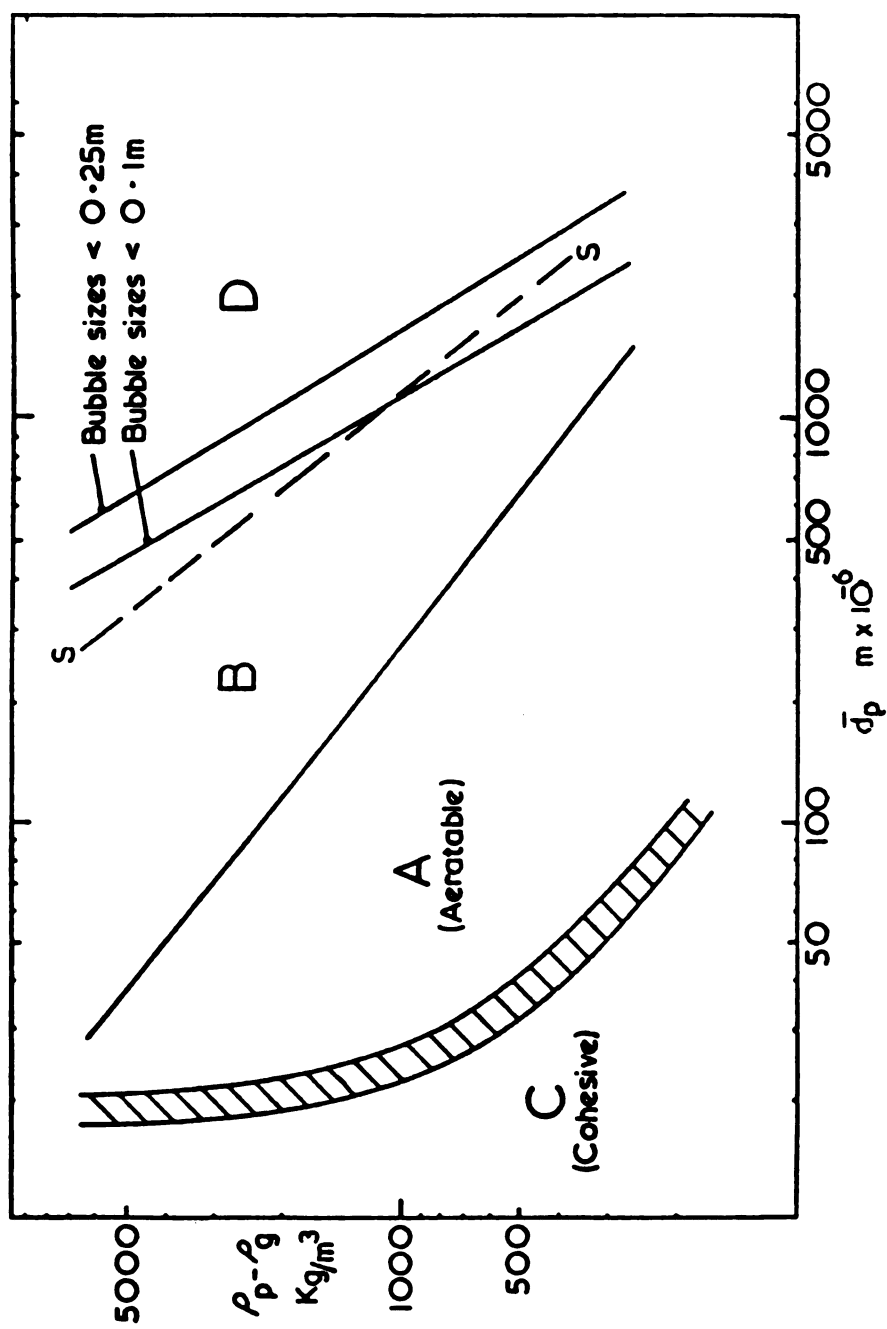


Figure 4.4 Characterization of fluidized powders by Geldart [14]

critical gas rate, "bubbles" of the gas form and move up through the powder bed. Type B powders are generally coarser than Type A powders. They begin "bubbling" at the minimum fluidization velocity and do not exhibit a homogeneous expansion. There are negligible interparticle forces in this category. Powders in the Type D category are generally the coarsest of solids and are dense and/or large. Due to their large size and high particle momentum, these powders do not exhibit any tendency to agglomerate. All cohesive powders fall into the Type C category and are very hard to fluidize. They also exhibit extensive agglomeration and large interparticle forces.

There is a general consensus of opinion that cohesion of dry powders is mainly due to Van der Waals forces [15]. This force operates both in vacuum and in a liquid environment, although in the latter case the Van der Waals forces is substantially reduced [16]. The Van der Waals forces are only noticeable when the particles can come sufficiently close together, on the order of the size of a molecule (0.2 to 1 nm). As the particle size increases, the gravitational forces begin to dominate. Therefore cohesiveness of powders is usually apparent when the particle sizes possess a major dimension of less than 10 μm .

In addition to the Van der Waals force, other attraction forces may also operate between the particles in a powder, such as capillary, electrostatic and magnetic forces. Table 4.1 lists the governing equations for each of these forces. Grace [17] has also pointed out that the boundary between A and C type powders is strongly influenced by the above forces as well as variables such as surface asperities, hardness of the solid material, humidity, melting or softening point, electrical conductivity, and magnetic susceptibility. In general, these forces are smaller than the omnipresent Van der Waals force.

Table 4.1 Governing equations of particle interaction forces

<i>Van der Waals force between two spheres,</i>	$F_w = \frac{AR}{12H^2}$
<i>Electrostatic force between two spheres,</i>	$F_e = \frac{Q^2(1 - \frac{H}{(R^2+H^2)^{3/2}})}{16\pi\epsilon_0 H^2}$
<i>Capillary force between two spheres,</i>	$F_h = 2\pi\gamma R$
<i>Magnetic force between two spheres,</i>	$F_m = \frac{p^2}{6\pi\mu H^2}$
<i>Force of gravity on a sphere,</i>	$F_g = 1.33\rho g\pi R^3$
<i>where A = Hamaker coefficient (dependent on the material);</i>	
<i>H = separation distance; ϵ_0 = permittivity of vacuum;</i>	
<i>Q = particle charge; γ = surface tension; μ = permeability;</i>	
<i>p = degree of magnetization; ρ = density; g = acceleration due to gravity</i>	

Electrostatic forces can contribute significantly to the cohesiveness of powders and thereby their agglomeration as long as a gaseous environment is considered. Triboelectric charging or the formation of a potential difference when particles of different work functions are brought into contact are the two major ways of development of electrostatic charge [13]. The former is due to the transfer of charge between similar particles due to friction. The latter occurs from a transfer of charge between dissimilar surfaces such as between the wall of the chamber and the powder particle. The agglomeration tendency of powder particles increases drastically with increasing surface area. This behavior has been noticed with the 5 micron powder that has been used in this investigation. The size of agglomerates varies from a few microns to 3 to 5 centimeters in diameter.

Figure 4.5 is a graph of the variation of the charge to mass ratio with specific surface area [18]. The results have been obtained by Glor, et.al. with a lab scale

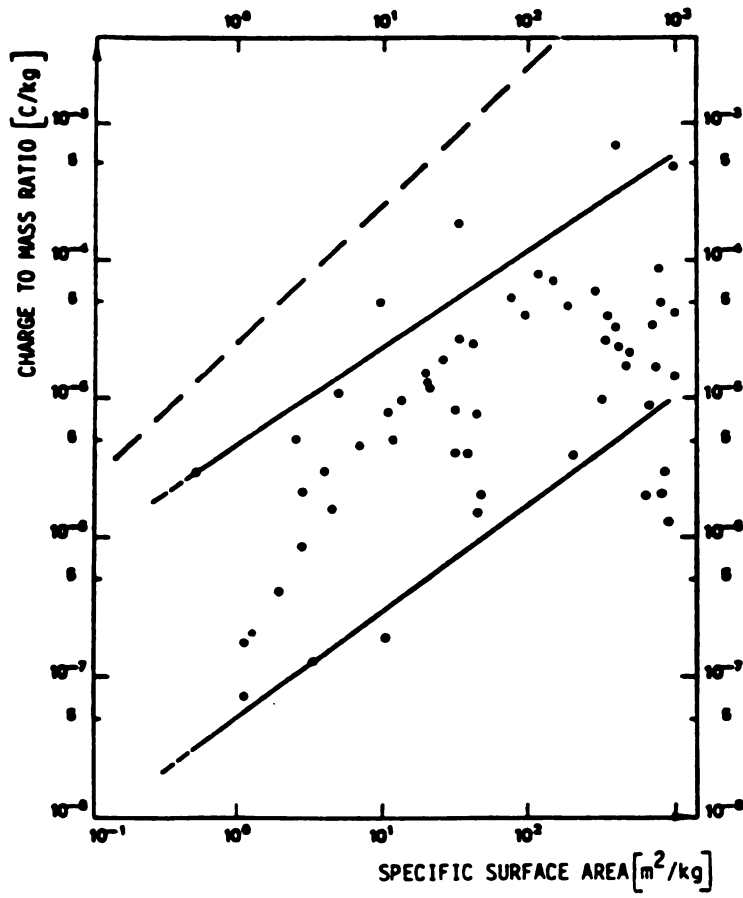


Figure 4.5 Trend of charge to mass ratio with specific surface area ^[18]

pneumatic transport device from many different organic powders of various substances of different particle size distributions. The overall dependence and trend of the charge to mass ratio is indicated by the two solid lines. This dependence is almost linear. The dashed line corresponds to the theoretical limit (based on the assumption of density = 10^3 kg/m^3 ; maximal surface charge density = $2.7 \times 10^{-5} \text{ Coulombs/m}^2$). For 5 micron powders, the charge to mass ratio would be significantly higher than for 10 or 20 micron powders because decreasing particle size causes an increase in specific surface area. Thus this powder would tend to be more cohesive. This is confirmed in the experiments where the 5 micron powder agglomerated extensively compared to either the 10 or 20 micron powders.

A number of methods were tried in order to reduce agglomeration. Initially, stainless steel ball bearings (5/16" diameter) were introduced into the aerosolization chamber along with the polymer powder. The choice of ball diameter was 5/16" because it was approximately the average size of the agglomerates in the chamber. The concept was to allow the balls to bounce around the aerosolizer and upon impact, break up the agglomerates. This technique was only partially successful. It reduced the size of the agglomerates but did not eliminate them. It was noticed that a number of fine agglomerates still existed in the chamber. Additionally, the spheres preferentially moved to the edges of the chamber due to the oscillation of the aerosolizer diaphragm and due to the presence of a vibration free, low energy node. Thus at the end of a given run, the balls were all found at the periphery of the chamber.

A second similar technique, reported by Sheehan and Carillo [19], involved using "hair-balls". These are metal spheres coated with some sort of fiber (e.g. cotton). They were used to disperse micrometer and submicrometer size particles (dust) in vacuum.

The hairballs serve several roles. They grind and mill the powder or dust particles. The bouncing balls break the Van der Waals and electrostatic bonds that bind the particles together. The fiber coating on the ball serves as a macroscopic solvent into which the dust dissolves before it is freed by impact. The fiber also serves as a cushioning which prevents damage to the diaphragm. The hairballs did not reduce agglomeration to a great extent. Observations revealed that the hairballs served as accumulation sites for powder. The fibers around the ball entrapped the powder and prevented their release into the aerosol. Thus the hairballs continually increased in size forming large agglomerates themselves. These agglomerates again accumulated at the low energy nodes around the periphery of the aerosolization chamber.

A third technique utilizing a 1/2" opening wire mesh was also tried. The rationale behind this method was to prevent agglomerates by the same mechanism as in the previous two methods but at the same time avoid the migration of the crushing medium to the chamber walls. The wire mesh was cut square to a size slightly smaller than the aerosolizer chamber. This allowed the mesh to move and rotate freely inside the chamber while at the same time vibrate with the powder. The mesh was successful in breaking some of the agglomerates. However, smaller size agglomerates still existed in the chamber. In addition, due to the differences in conductivity of the mesh and powder, the mesh was coated with the powder during the course of a run. Over long periods of time the mesh openings would close.

Since the technique of physically breaking the agglomerates was not entirely successful, a different approach was tried. This involved changing the conditions of the medium surrounding the powder particles. Initially dry nitrogen gas was used. The gas was allowed into the chamber at the bottom of the chamber. No significant change was

noticed in the agglomeration behavior. A humidified nitrogen supply was then substituted. This was achieved by bubbling dry nitrogen through an flask of distilled water. No noticeable difference was observed in the size of the agglomerates.

A fifth technique of drying the powder before aerosolization was also tried. The powder was heated in a pan for 10 minutes at 125 °C. The dry powder was immediately put into the aerosolization chamber and a positive nitrogen gas supply was started. This was done in order to prevent any back diffusion of moisture into the chamber. The aerosolizer was then run for about 30 minutes. This technique did reduce the size of agglomerates to around 0.5 mm diameter. Moisture is thus an important factor in agglomeration. It tends to accumulate and form hydrogen bonds with the organic molecules on the surface of a polymer particle. The free ends of the water molecules on adjacent particles can also form hydrogen bonds. Thus a number of particles can associate together and form agglomerates. The last technique described reduces the moisture content on the surface of the particle and thus reduces agglomeration. It therefore seems to be the most feasible solution to the problem of agglomeration. This modification should be incorporated into future systems where the powder would be continuously dried before feeding into the aerosolization chamber.

4.4 Particle Concentration Measurement

Aerosol concentration is an important design variable needed for scale-up of the prepreg process. In order to measure this a Realtime Aerosol Monitor (RAM-S) is fitted online with the system. The operating principle [20] of the RAM-S is based on the detection of the near-forward scattered electromagnetic radiation in the near-infrared. Figure 4.6 is a schematic of the system. Samples of the powder in the aerosol chamber are conveyed to the RAM-S through a copper tube. The optical detection unit in the

RAM-S measures the scattered radiation and coupled with the flowrate of the aerosol stream calculates the concentration. However, due to the inherent cohesive nature of polymer powder the measuring system gets fouled. The instrument zero drifts after a short sampling period. This causes large errors in the readings.

Since powder charging is the one of the primary reasons for fouling, a possible solution would be the introduction of an online deionizer unit that would neutralize the charge on the polymer particles. This must be considered in any future scale-up systems that are planned.

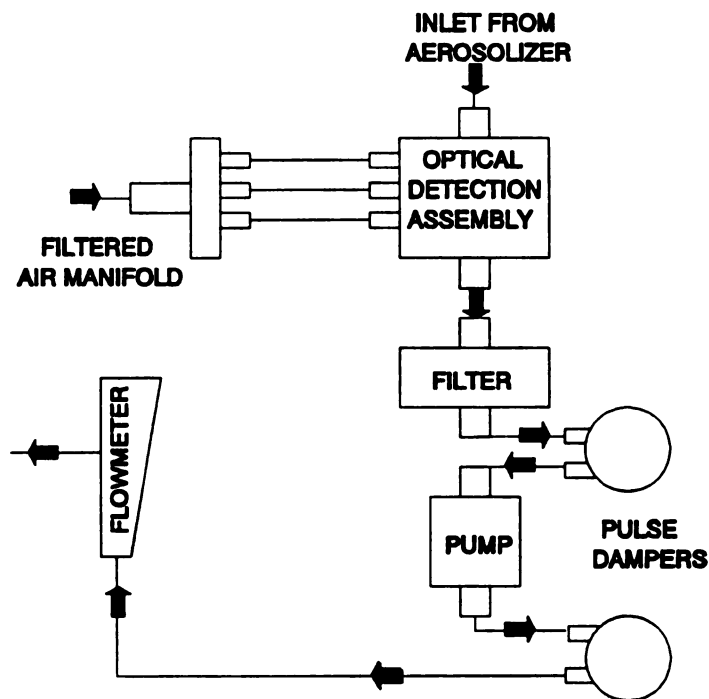


Figure 4.6 Schematic of Real-time Aerosol Monitor

Chapter 5

PROCESS MODELLING

A number of variables affect the powder prepegging operation. A model that incorporates these variables would aid in understanding their effect on the process. Three main areas of the powder prepreg process can be identified for the purposes of modelling : the spreader, the aerosolizer and the sintering oven. The last two have been characterized physically [4]. The aim of this chapter is to develop a model for the spreading operation.

5.1 Choice of Modelling Technique

Three approaches to the modelling are possible. A purely theoretical method could be followed which involves determining the individual forces and parameters and then using fundamental principles to develop a mathematical representation for the unit operation. This requires a thorough knowledge of the fundamental quantities and forces that are involved. The operation of spreading is mathematically not well understood and hence this method would be quite difficult.

Another method which would be the other extreme of modelling involves generating data from the experimental setup and then using a graphic software package to fit the data to a curve. This would give a mathematical model that describes the

process but does not indicate the physical parameters. This technique is therefore empirical in nature and would be the easiest of the three techniques.

A third technique falls between the above two categories. This is semi-empirical and gives a more realistic picture of the physical situation than the purely empirical approach. Dimensional analysis is a method that falls under this category [21]. In order to apply this technique, one needs to know only the variables believed to be involved and their dimensions. With the use of fundamental algebra, and in some cases without any experimental data, this method can predict the effect of a variable on the model. However, this method will not give any quantitative information and experiments must be conducted in order to quantify the model.

Dimensional analysis tries to group all the variables involved into dimensionless groups. There are two techniques that have been used :

- a) Rayleigh method
- b) Buckingham Pi method

The Rayleigh method is the simpler of the two since there is no necessity of knowing the number of dimensionless groups beforehand [21]. It has been used in literature to model material properties and processes [22]. Thus it was chosen for the purposes of this modelling.

5.2 Model Development

Rayleigh's method is based upon the premise that if n quantities, $Q_1, Q_2, Q_3, Q_4, \dots, Q_n$, are involved in a certain physical phenomenon, for the purpose of the dimensional analysis their mutual dependence may be expressed as a power product of the following type:

$$Q_1 = K (Q_2)^{a_2} (Q_3)^{a_3} (Q_4)^{a_4} \dots (Q_n)^{a_n} \quad (3)$$

where K is a dimensionless constant. By introducing the fundamental units of the n quantities and by using the condition of dimensional homogeneity, the constants $a_2, a_3, a_4, \dots, a_n$ can be determined absolutely or related to each other. The relationships can then be rearranged to give dimensionless quantities.

Table 5.1 Parameters involved in spreader modelling

Parameter	Description	Base units (Mass, Length, Time)	Comments
W	Watts	ML^2/T^3	Related to amplitude (rms Volts).
f_o	Frequency	1/T	Term incorporating applied frequency and resonant frequency.
A	Fiber adhesion	M/T^2	Adhesion existing between fibers due to sizing, etc.. Will be zero for bare fiber. Units of energy/ area.
n	Tow size	none	Number of fibers / tow.
D	Fiber diameter ratio	none	Ratio of diameter of fiber to a standard fiber (AS4 carbon fiber).
p	Number of rods	none	-
ϵ	Friction coefficient	none	Friction between fiber and rod.
S	Spread width	L	Primary variable

The first step in the analysis is to list all the parameters involved in the physical situation along with their fundamental units. The parameters for the spreader are listed in Table 5.1. The motivation for the development of the model is to relate the spread width of the fiber tow to physically observable parameters.

By equation (3) that describes Rayleigh's method,

$$S = KW^a f_o^b A^c n^d p^e \rho^f D^g \quad (4)$$

where K is a dimensionless constant.

Substituting the dimensional base units for each parameter in equation (4),

$$L = \left[\frac{ML^2}{T^3} \right]^a \left[\frac{1}{T} \right]^b \left[\frac{M}{T^2} \right]^c \quad (5)$$

Using the condition for dimensional homogeneity, i.e., all the units must balance in an equation,

$$\Sigma M = 0 \quad : \quad a + c = 0 \quad (6)$$

$$\Sigma L = 0 \quad : \quad 2a = 1 \quad (7)$$

$$\Sigma T = 0 \quad : \quad -3a - 3b - 2c = 0 \quad (8)$$

Solving equations (6), (7) and (8) for a, b, and c, $a=0.5; b=c=-0.5$.

Resubstituting these values in equation (4),

$$S = KW^{0.5} f_o^{-0.5} A^{-0.5} n^d p^e \rho^f D^g \quad (9)$$

Rewriting equation (9),

$$S = K \left[\frac{W}{f_o A} \right]^{0.5} n^d p^e \epsilon^f D^g \quad (10)$$

which is the desired relationship of spread width to the parameters.

This model predicts that the spread width goes as the square root of the amplitude (or watts) and is inversely proportional to the square root of inter-fiber adhesion. It also postulates that the spread width is inversely proportional to the frequency parameter, f_o . This parameter needs to be defined and must incorporate the resonant frequency, f_r , of the system. The definition also needs to ensure that physical data collected from the spreader fit any curve predicted by the model. A simple definition was considered as a first approximation and is given by equation (11).

$$f_o = \frac{(f-f_r)^2}{f_r} \quad (11)$$

The square of the numerator was chosen to give f_o the units of frequency. Substituting equation (11) in equation (10),

$$S = K \left[\frac{W}{A} \right]^{0.5} \left[\frac{f_r}{(f-f_r)^2} \right]^{0.5} n^d p^e \epsilon^f D^g \quad (12)$$

Data from spreading experiments of AS4 carbon fiber [23] are listed in Tables 5.2 and 5.3. The data shows a trend similar to that predicted by the model. The model predicts that the spread width goes to infinity as the frequency approaches resonant conditions. Physically this translates into a maximum for the spread width. The model also describes a square root curve for amplitude. From the data it can be seen that the spread width almost plateaus out with increasing amplitudes thus closely following the model. Figure 5.1 graphically displays the trend of the spread width as frequency is

varied. The data from Table 5.2 has also been plotted. All the parameters from equation (12) except for frequency have been combined into a single parameter which has a value of 5.53. This value has been arrived at by visually best-fitting the data to the model. The value of the individual parameters is however not known. A value of 35.5 hz has been chosen as the resonating frequency of the spreader unit that was used to obtain the data. Figure 5.2 is a similar representation of the variation of spread width with amplitude. The single parameter is now made up of different individual parameters and has a value of 2.29. From these two graphs it can be seen that as a first approximation the model fits the data reasonably well.

Though data from spreading of fibers with different inter-fiber adhesive strengths has been obtained, they are not listed because of the inability to quantify inter-fiber adhesion. The trend indicated by the model is that of decreasing fiber spread with increasing inter-fiber adhesion which is to be expected.

Thus, a very simple model has been developed which describes some of the trends of the spreading operation. Further data acquisition and analysis is required in order to fit the model better to the observed values. The model is not perfect and is only an indicator of the performance of the spreader. Further refinement of the model is necessary to enable practical use of it. The effects of the remaining parameters, for which coefficients have not been determined, must be investigated. Finally, in order to complete the model scaled-up spreaders should be used to determine its effectiveness.

Table 5.2 Spreading experiments on AS4 carbon fiber at constant amplitude, varying frequency

No.	Frequency	Amplitude	Spread Width
	Hz	rms Volts	cm
1	21.1	10.5	0.5-4
2	25.3	10.7	3-7
3	30.0	10.5	4-9
4	32.1-32.4	10.5	5-9
5	34.3	10.5	5-9
6	36.1	10.6	6-9
7	38.3-38.4	10.5	5-9
8	40.0	10.5	4-7
9	42.2	10.5	2-6
10	44.1	10.5	0.5-5

Table 5.3 Spreading experiments on AS4 carbon fiber at constant frequency, varying amplitude

No.	Frequency	Amplitude	Spread Width
	Hz	rms Volts	cm
1	36.3-36.4	4.7	0.5-4
2	36.3	7.6	4-7
3	36.3	9.8	6-9
4	36.3-36.4	10.1	7-9
5	36.1	10.6	6-9
6	36.0	11.8	7-9

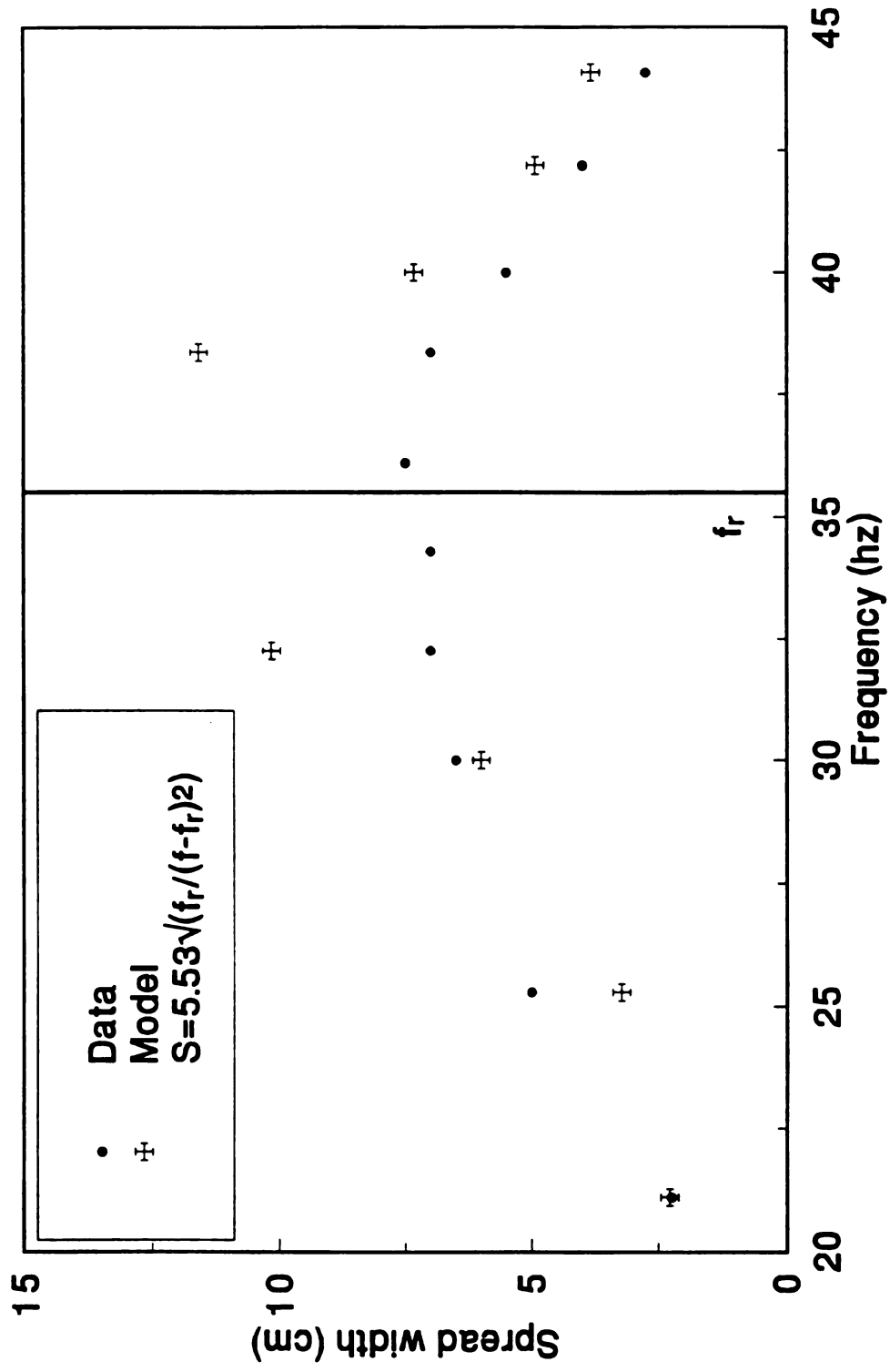


Figure 5.1 Comparison of model and data of spread width versus frequency

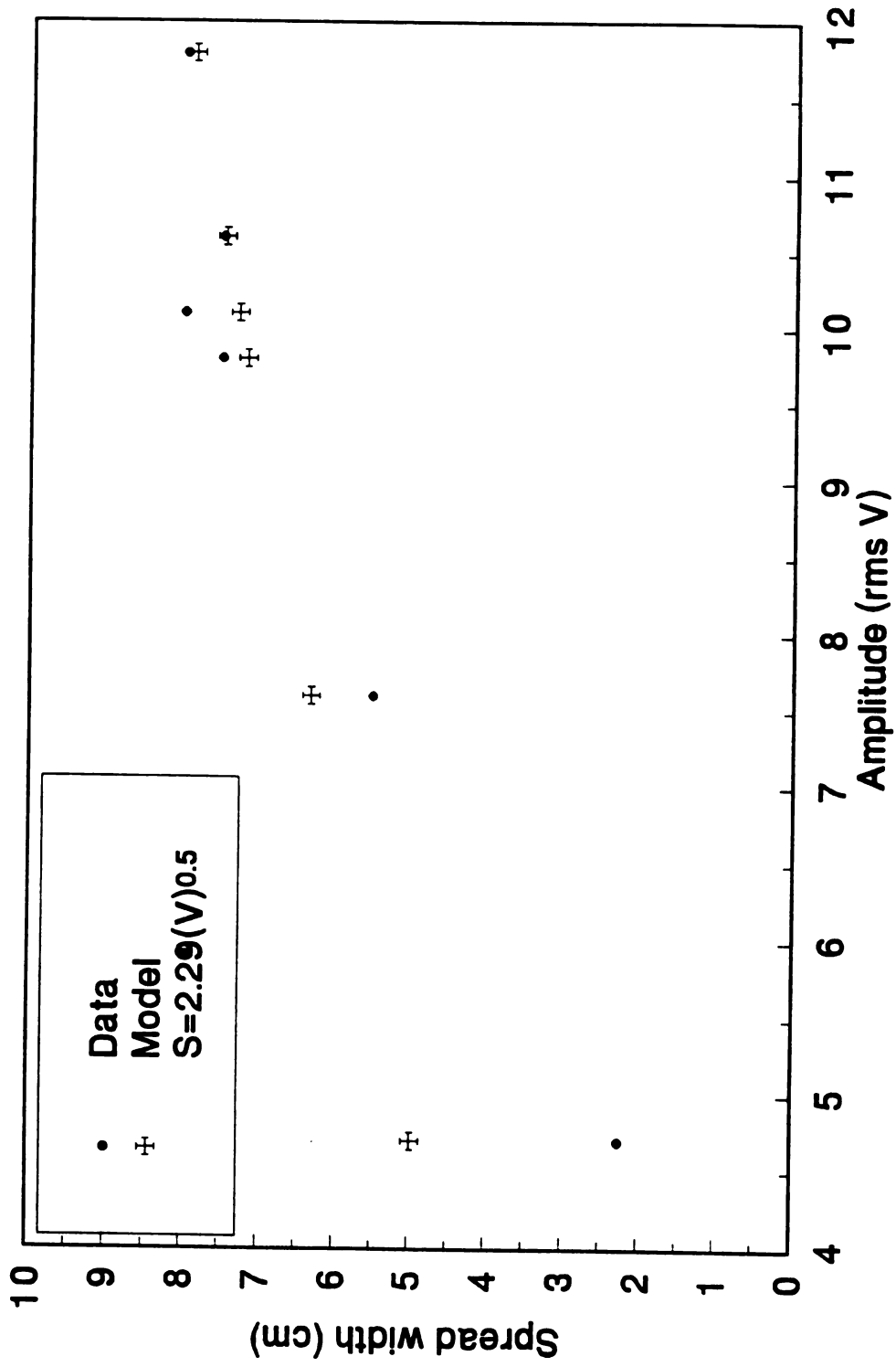


Figure 5.2 Comparison of model and data of spread width versus amplitude

Chapter 6

PARTICLE SIZE EFFECTS

Two different areas of the powder prepreg process were examined in this investigation. The first was to determine the effect of particle size on the operation of the system. The second was to develop new applications for the process. Chapter 6 describes the particle size effects while new applications are discussed in Chapter 7.

The particle size is a variable in the process. Its effect on the system could be in two separate domains :

- a) It could affect the manufacturing conditions of the prepreg tape.
- b) It could change the processing characteristics of the prepreg tape.

As described in Chapter 2, the manufacture of the prepreg tape involves unwinding of the fiber tow, spreading it into individual filaments, depositing polymer particles from an aerosol onto the fiber, sintering the individual powder particles in place and finally winding the prepreg tape onto a spool. The processing of the prepreg tape involves cutting up the tape, laying it up in a mold and then applying heat and pressure in a controlled cycle to get a final void-free composite part. It was the hypothesis of this investigation that change in particle size would affect powder deposition and polymer pick-up as well as sintering times. It was also thought that the consolidation pressure needed to get a void-free part would be related to particle size. The experiments that have been conducted were to assess these effects.

6.1 Prepregging Experiments

The experimental procedure followed for this section was as follows. The aerosolizer chamber was removed and cleaned with alcohol to decrease the number of high surface energy areas. The aerosolizer was replaced and charged with 225 grams of the polymer powder under investigation. The required process variables were then set. The operating frequency of the aerosolizer was determined by visual observation of the diaphragm. The operating frequency corresponds to the natural frequency of the chamber and is the point where the amplitude of oscillation of the diaphragm is maximum. The process was started through the control software and allowed to run for 15 to 20 minutes to achieve a steady state. A piece of masking tape was used to mark the starting point for the run on the prepreg tape. The run was allowed to proceed with the least possible manual intervention. Manual checking was necessary from time to time due to the variation in the line speed control and involved slowing down the take-up drum so that the tow tension was maintained. Fluctuations in the tow tension caused changes in tape width and consequently in the volume fraction of the prepreg tape. The total run time for most experiments was approximately one hour.

The prepreg tape that was produced was cut into 32" lengths. Ten lengths were laid together to form a batch. Three lengths (#1, #4 and #7) from every batch were weighed accurately. These weights were entered in a spreadsheet (SuperCal4). The average weight of an uncoated 32" length carbon fiber tow was also recorded. An average volume fraction for the run was calculated using the technique described in Section 2.3.1.

Table 6.1 Results of prepegging experiments

Size	Spreader		Aerosolizer		V _m	Standard Deviation
	Freq	Amp	Freq	Amp		
Microns	Hz	V	Hz	V	%	± %
5	38.5	11.0	12.4	5.90	17.8	3.2
				7.25	14.2	4.8
				9.00	19.0	6.5
				11.15	27.2	4.3
10	38.5	11.0	12.5	5.90	35.0	5.9
				7.25	38.9	6.4
				9.00	39.6	5.7
				11.15	47.6	4.5
20	38.5	11.0	12.5	4.25	10.1	3.1
				5.90	14.4	4.6
				7.25	23.8	4.0
				9.00	31.3	3.1
				10.00	37.6	4.5
				11.15	39.5	1.4
65	38.5	11.0	12.3	5.90	3.1	2.0
				7.25	3.4	3.7
				10.00	5.4	3.9
				11.15	7.6	3.4
				15.40	12.0	3.1

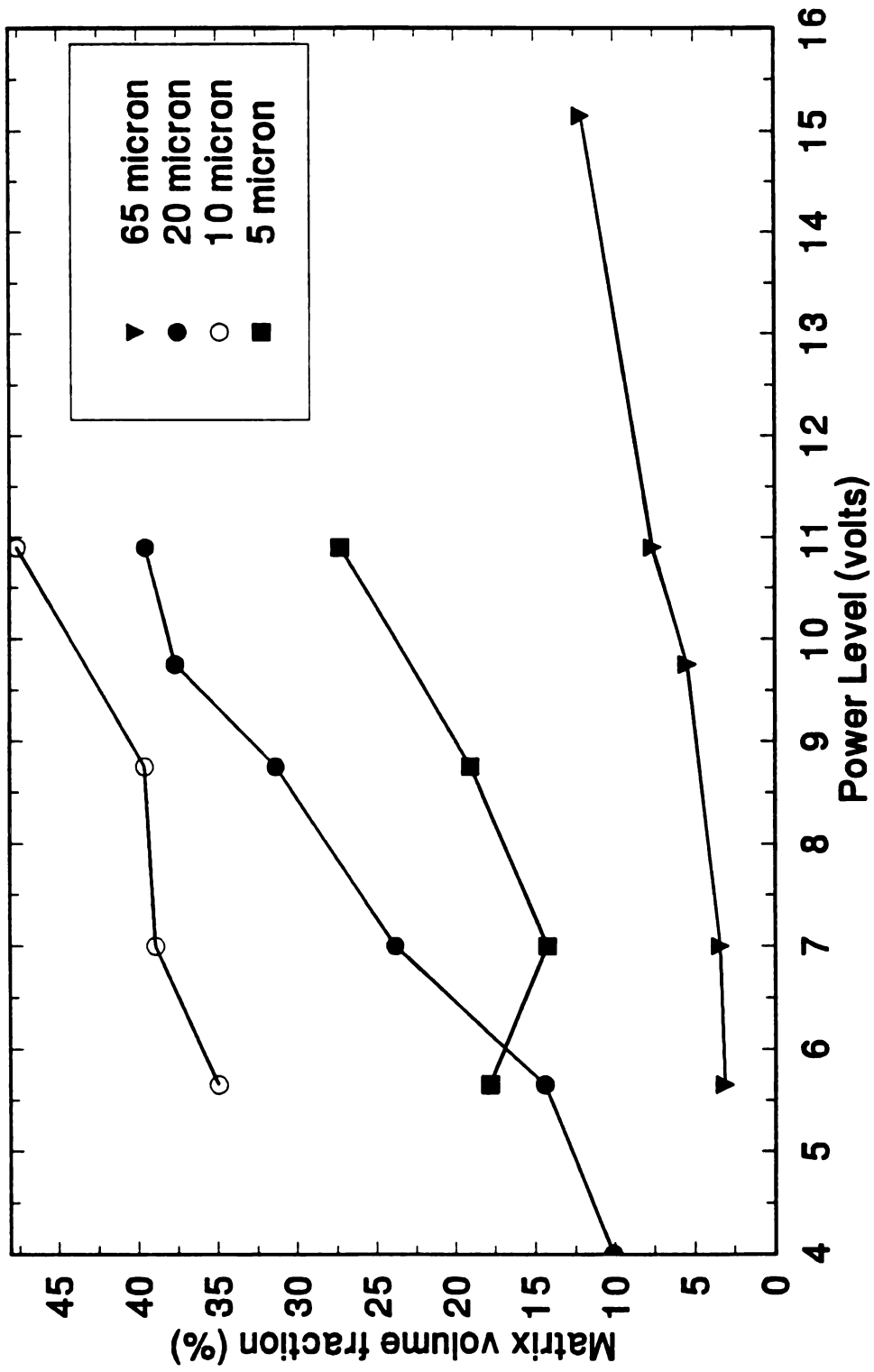


Figure 6.1 Variation of V_m with amplitude

The experiments were conducted on the 5, 10, 20 and 65 micron powders at different voltage (amplitude) levels. The results of these experiments are tabulated in Table 6.1. In Table 6.1 the amplitude and frequency have units of volts (V) and hertz (Hz) respectively. The term V_m refers to the volume fraction of matrix (polymer) present in the prepreg tape. The results tabulated in Table 6.1 are graphically displayed in Figure 6.1. It is seen that the data for the four different particle sizes is significantly different. The standard deviation of each point is extremely small i.e., any given point can be repeated to within 5% of the stated value [24]. This fact has also been confirmed through independent observations. The general trend is that as amplitude (and therefore power) is increased, there is an increase in aerosol generation leading to increased polymer pick-up. As the pick-up increases there is an increase in the matrix volume fraction which is the y-axis of the plot in Figure 6.1.

The volume fraction of the 65 μm powder shows an almost linear relationship with amplitude. However, the pick-up is extremely small and reaches only 12% by volume even at significantly high amplitude levels. The 20 μm powder follows a similar trend but attains higher pick-up percentages. The operating line is higher and a wider range of volume fractions can be achieved with this powder. The 10 μm powder operating line is higher than the 65 μm and 20 μm lines and this gives much more flexibility in operation of the powder prepreg system. The 5 micron powder shows a trend opposite to that which is observed for the other size ranges. It is lower than the curves for the 10 and 20 μm powders.

Two important conclusions can be drawn from the above observations. First, larger particle sizes, because of their increased weight, require considerably higher amplitudes (and hence energy) in order to fluidize. The amplitude of the input signal

drives the speaker which in turn vibrates the diaphragm and the particles present on it. Physically, an increased energy input to the aerosolizer translates into an increased amplitude of oscillation of the diaphragm and hence an increased upward buoyancy force on the powder particles. This causes larger powder particles to aerosolize and move upwards through the chamber where they can intersect the spread fiber tow. Thus, for the same energy, more 10 μm particles intersect the fiber than 20 μm particles. This results in approximately 10 V_m % higher pick-up in the case of 10 μm powder compared to 20 μm powder. In the case of the 65 μm powder this difference is approximately 30%. The operating line is much lower and hence would represent an upper limit on particle size for the present system.

The second conclusion that can be drawn is that a lower size limit exists for the system. This can be observed from the 5 μm curve. Theoretically, it would be expected that the 5 μm operating line lie above the 10 μm curve since the particle size is smaller (because less energy is needed for aerosolization for smaller particle sizes). However, this is not the case observed in the experiments. The reason for this is the extensive agglomeration that occurs in the aerosolization chamber due to the high charge to mass ratio of the 5 μm powder particles. The size of agglomerates increases to approximately 3 centimeters within 10 - 15 minutes of a run. These agglomerates require higher energy levels to fluidize and this leads to much poorer pick-up. The curve of the 5 μm therefore lies approximately where a 35 μm powder operating line would lie.

These results on the effect of particle size would indicate that a critical size range exists with the present carbon fiber - polyamide system. Below or above this size range the operation of the system is unsatisfactory because of poor pick-up. In the case of the present system this critical size range is approximately 5-20 μm . Pick-up percentages

in the range of 0-15 % by volume of matrix is undesirable since prepreg tape of this volume fraction cannot be consolidated to give a void-free part. The theoretical limit of V_m for a void-free consolidated part is 9.8% [25]. Therefore any prepreg tape that is to be consolidated to get void-free parts needs to have atleast this percentage of matrix already present. In addition a small amount of matrix is lost due to bleeding during the consolidation process. The above factors impose limits on the powder sizes that can be used effectively in the present system. However, these limits vary from one fiber-matrix system to another. In order to successfully utilize the powder prepreg system, operating windows dependent on particle size and charging properties must be established for each fiber-matrix combination.

6.2 Consolidation Experiments

The second part of the investigation involved the effects of particle size on consolidation. One of the important advantages of the powder prepreg system over other systems is that the melt viscosity of the polymer has less importance than the other variables. The polymer has to flow over only very short distances (in the order of Angstroms rather than millimeters) for consolidation. This would not be the case when particle size is increased in the consolidation step when the large particles must melt and fuse with the rest of the matrix. Thus it is important to quantify the role of particle size in the prepreg tape as to whether processing of larger particle sizes would require higher consolidation pressures to form void-free parts and whether the consolidation pressure has to be higher for higher fiber volume fraction tape since the small fraction of matrix needs more force to flow over the entire composite part.

The experimental program for this section involved making the prepreg tape with a particular particle size. The volume fraction of the tape was estimated as described in

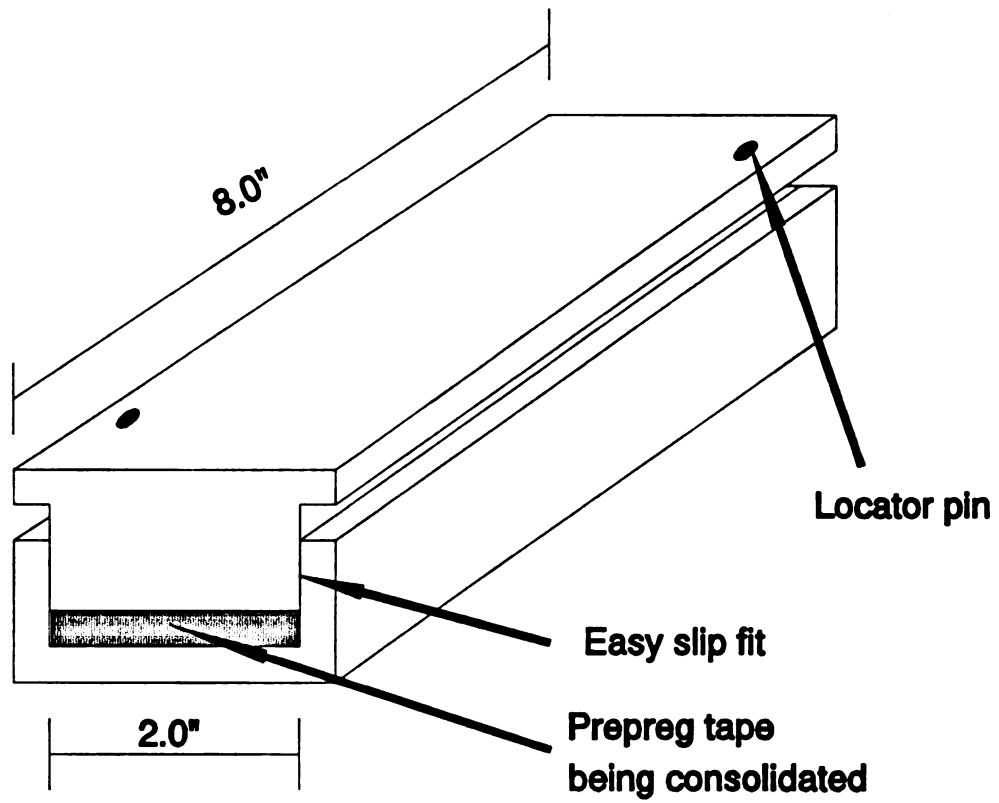


Figure 6.2 Schematic of consolidation mold

Section 2.3.1. This value formed the x-axis for a plot of consolidation pressure versus volume fraction. The entire length of tape from the run was divided into three equal parts. Each part was cut up into 4" lengths and laid up in an unidirectional fashion in a two-part open-ended mold illustrated in Figure 6.2. A base pressure was determined from a graph of consolidation pressure and V_f for the 10 micron powder [26]. This was used as a reference point. The three parts were individually consolidated at three different pressures - one below, one above and one at the base pressure. The consolidation cycle used has already been illustrated in Figure 2.5. Sections from the composite part were cut using a diamond saw, mounted in acrylic holders and polished down to 0.05 micron grit as described in Section 2.3.3. The volume fraction and void fraction were determined optically using the ONVFA [8]. The consolidation pressure used and the volume fraction are plotted as the y and x - axis respectively. An operating curve was drawn which divided the graph into two regions. Any point above the operating curve represented a part which showed bleeding (matrix oozes out) and was void-free. A point below this curve represented parts that had voids. This plot is shown in Figure 6.3.

It can be seen from the graph that the operating lines for the three particle sizes are quite close and even overlap. Within limits of experimental error all three curves are essentially the same. This would indicate that the consolidation pressure needed to make void-free composites is independent of the particle size over the range of 5 to 20 μm . It must however be recalled that the melting times of polymer particles varies from seconds to minutes depending on particle size. Thus any differences in processing that depends on particle size will manifest themselves in this time frame. Beyond this the polymer is basically a melt and will be a viscoelastic fluid. The consolidation times used in the experiments are on the order of 30 minutes (heating) which exceeds the maximum

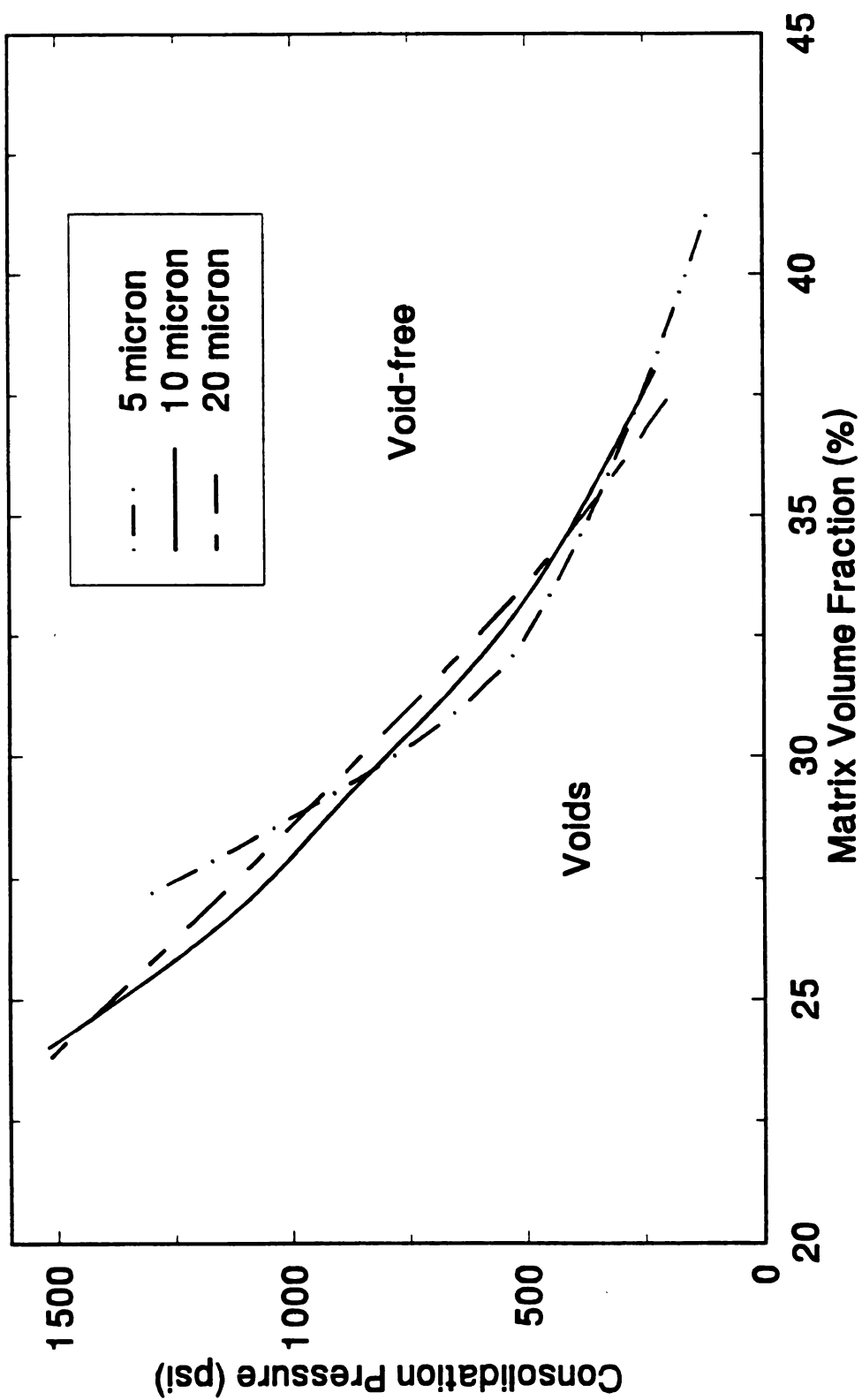


Figure 6.3 Plot of consolidation pressure versus V_m

time required for consolidation. Thus any differences between particles is wiped out, accounting for the similarity in the three curves.

In order to study the differences in processing as a function of particle size, it would be necessary to conduct consolidation experiments of shorter durations. The time of consolidation should be varied at constant pressure to determine the minimum consolidation time. Another factor that has to be considered is the thickness of the consolidated sample. If thick samples are used for consolidation, the time for heat transfer may be far greater than the time for melting. This would lead to uneven consolidation in the part. So a probable experimental plan would be to choose three different sizes of powders (preferably in the 5 - 100 μm range) and make fixed matrix volume percent prepreg tape from them. These tapes should be laid up and consolidated at different pressures for variable amounts of time into thin samples. A void analysis on these samples would give data points through which an operating line for consolidation pressure could be drawn. This line would separate the samples with voids from those that are void-free and would quantify the effect of particle size on processing.

The above two experimental programs have showed that for the AS4 carbon fiber - polyamide system :

- a) The effect of particle size is significant and must be considered when any sort of scale-up is made.
- b) For the consolidation cycles being used, at long processing times there is no significant differences between the prepreg tapes made from different particle sizes. However, the relationship between processing speed and particle size has not been established.

- c) **A critical size exists for this process with these materials for which powder prepegging by the present process is unsatisfactory.**

Chapter 7

NEW APPLICATIONS

The powder prepreg process is a combination of four unit operations : spreading, aerosolization, impregnation and sintering. The individual steps of this process can also be adapted to other applications. This chapter describes two of the new applications that were successfully tried.

7.1 RTM Preform Manufacture

Resin Transfer Molding (RTM), also called "liquid molding", is a process for obtaining a product with two relatively good appearing surfaces with better dimensional control than other open mold processes [27]. In this process, the reinforcement, without the resin, is loaded into the mold, the mold is closed, and the resin is injected or transferred into the mold, in such a manner as to completely impregnate the enclosed reinforcement. One of the problems facing this process is the shifting of the reinforcement (or preform) during the injection of the resin. This leads to a bunching or nesting of the fiber reinforcement in certain areas of the mold. This reduces the interstitial space necessary for easy resin flow and consequently there is lesser amount of resin in these areas of the mold. These areas are called "bald spots" and are undesirable due to the uneven mechanical properties they result in. Any mechanism to hold the preform in place would therefore be beneficial. One possible way to temporarily hold the fibers fixed in space is to use thermoplastic particles to act as welding agents between different

layers of reinforcement. The powder prepreg process has the advantage of being able to produce continuous fiber tape with any desired thermoplastic matrix volume fraction and therefore could be a method to produce RTM preforms.

The procedure to make these preforms involved operating the powder prepreg process at low aerosolizer amplitude levels. AS4 carbon fiber and polyamide were the materials used. A particle size of 20 microns was used in the aerosolizer and temperatures of 160-170 °C were used in the sintering stage. The powder was sintered to the fiber only at points of contact. Due to the low temperatures being used, the tape remained quite flexible and tacky. This gave prepreg tape of very low matrix volume fractions (of the order of 5 to 10% by volume) with the polymer powder almost maintaining its original spherical shape.

The tape was then wound around a complex, three dimensional mold shape. For the purposes of this study, a bottle with a square cross-section was used. The tape was heated with the mold to the melt temperature of the polyamide with a heat gun or by placing it in a convection oven for 4-5 minutes. The mold was allowed to cool and the preform was removed. This gave a stable three dimensional reinforcement that retained the shape of the mold. A photograph of the mold and the preform is shown in Figure 7.1.

Figure 7.2 shows an SEM photograph at 200 X of a section of the preform. Two important characteristics can be noticed from the micrograph. First, the polymer acts as a uniformly distributed spacer between the individual fiber filaments holding them firmly in space. This gives good porosity in the reinforcement allowing high mass transfer rate and even wet out. Second, even though the fraction of thermoplastic

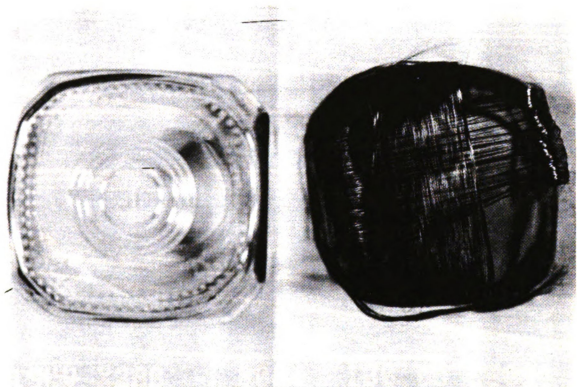


Figure 7.1 Photograph of mold with preform

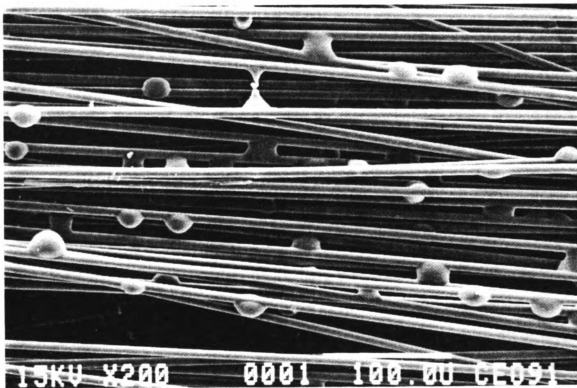


Figure 7.2 SEM photograph of RTM preform

polymer is quite small the axial distance between individual droplets of polymer is not very large. The inherent stiffness of carbon fiber supported over such small lengths would thus prevent any significant deformation of the fiber during high pressure transverse flow with viscous resins.

This study has shown that thermoplastic particles can be successfully used to act as spacers for a RTM preform. The choice of thermoplastic polymer is dependent on the resin used during the RTM process. The thermoplastic particles are temporary and can be burnt off during resin impregnation. This would reduce the contamination of the final part with thermoplastic polymer. Thus the thermoplastic particles help in holding the preforms in place till such time the impregnated resin gels and prevents any movement of the fibers within the part.

7.2 Impregnation of Fillers

Fillers, such as solid glass beads, have been used since the early seventies to improve toughness of glassy SAN copolymer [28]. The addition of hollow fillers has been of interest recently, especially in automotive applications. These fillers result in weight savings of nearly 25% depending on the application. The impregnation of hollow glass spheres into random glass fiber mats was an application that was explored during this study.

The properties and sources for the materials involved have already been listed in Chapter 3. Other techniques of impregnation (such as mixing of spheres with resin before injection into a RTM mold) have not been completely successful. The glass fiber mat acts as a filtration device for the spheres and this results in accumulation of the spheres near the gates of the mold. The idea behind this work was to develop a

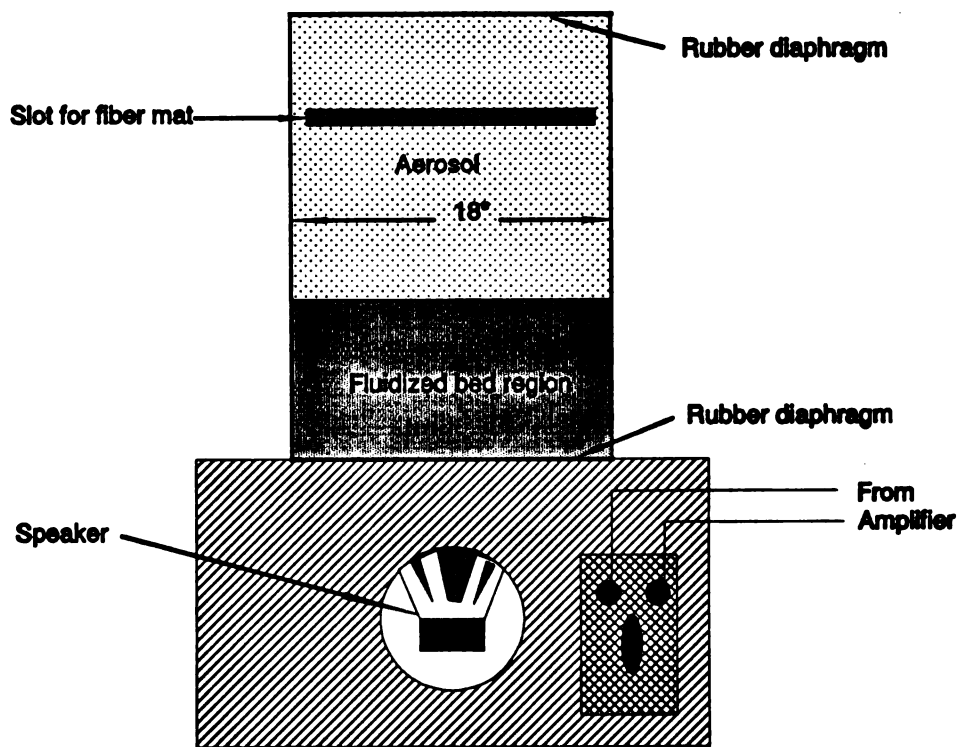


Figure 7.3 Schematic of aerosolizer for filler impregnation

technique that utilizes the impregnation capabilities of the powder prepreg system to evenly distribute the glass spheres into the fiber mat prior to resin injection.

The setup consists of an 18" diameter aerosolizer that is capable of impregnating 12" x 12" square mats. A schematic of the aerosolizer is shown in Figure 7.3. It is similar to the aerosolizer used in the powder prepreg process. The differences are in the size and that there is only one slot for the fiber mat (Although a batch type operation was used here, the process could be made continuous). The mat which is cut from a roll, is placed in an aluminum frame that fits through the slot and rests on two supports inside the chamber. The entire chamber can then be sealed by taping the slot.

The aerosolizer was charged with 525 grams of glass spheres. This gave a bed height of approximately one inch. Before actual impregnation could be done, the optimum frequency and amplitude of the system with all its components had to be determined. To determine these parameters, a sample mat was placed in the aluminum frame and then placed inside the chamber. The process was operated at different frequencies and amplitudes and the fluidized bed height was recorded in each case. The bed height was plotted against frequency for different amplitudes (voltage levels) as shown in Figure 7.4. The values for the amplitudes are only relative and are the dial settings on the amplifier. It can be noticed that there is a peak in the bed height at almost the same frequency for each curve. This frequency corresponds to the resonating frequency of the system. The amplitude does not affect the bed height to a great extent.

The impregnation of the fiber mat with spheres involves operating the process at the optimum frequency and amplitude with the mat placed inside the chamber. Impregnation time depends on the weight of spheres needed on the mat. Typically, a 5-6

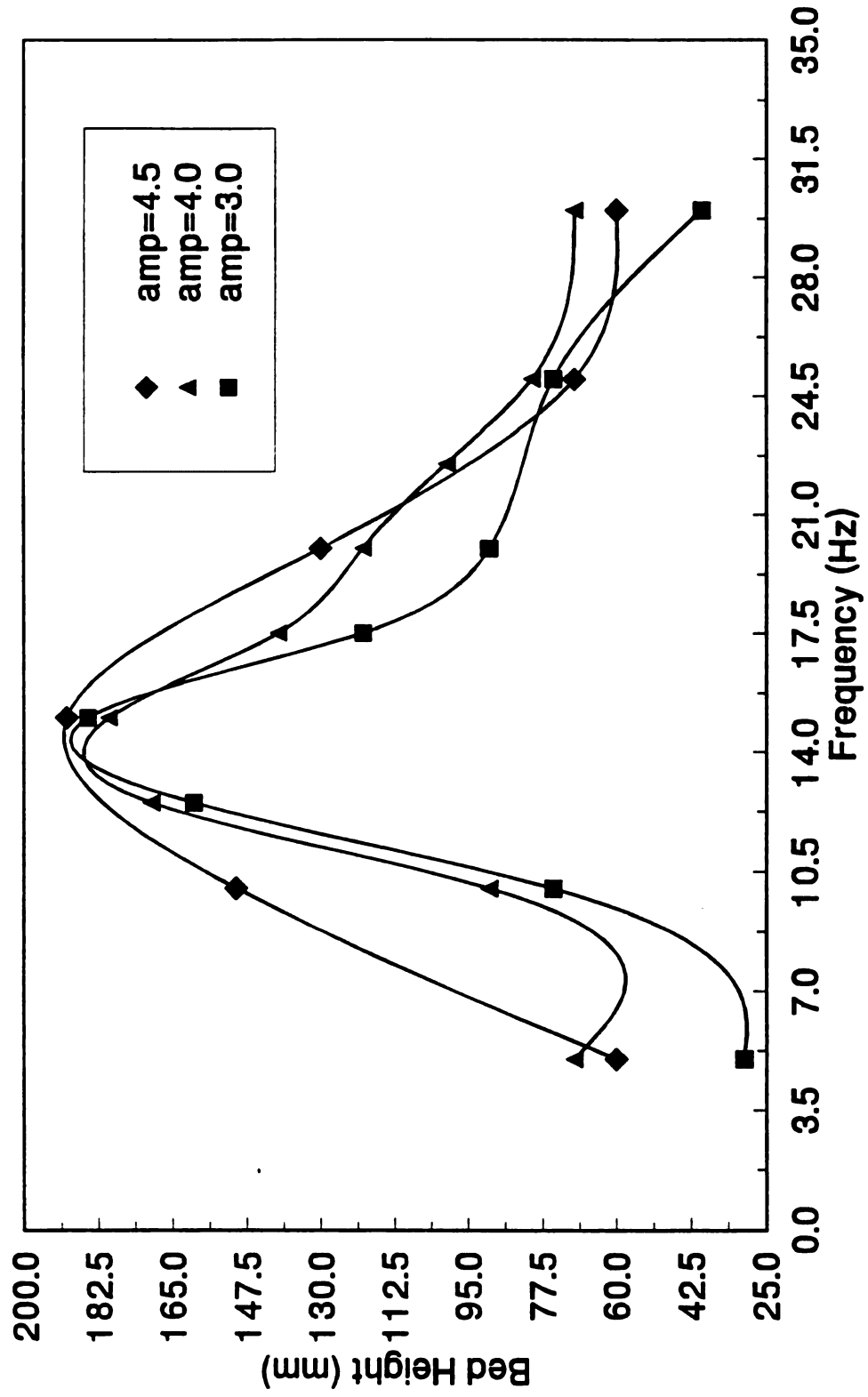


Figure 7.4 Frequency versus bed height at various amplitudes for 18" diameter aerosolizer. (Amplitude values are relative)

minute run would give 10% by weight of spheres on the mat. This would result in a weight savings of approximately 25%. Table 7.1 lists the parameters and weights for a typical run.

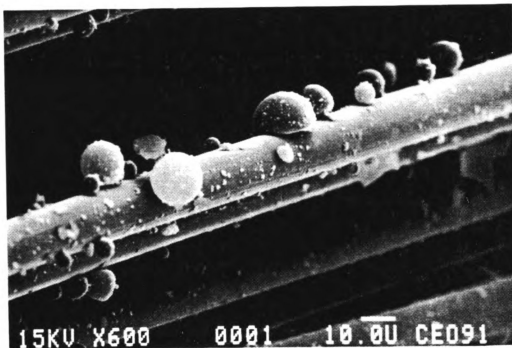
Though the impregnation process is successful, the spheres adhering to the mat are not fixed strongly enough to withstand normal handling. They are held to the glass fibers by very weak forces. Figure 7.5 is an SEM photograph at 600X of the glass spheres on a typical glass fiber. It appears that the spheres just sit on top of the spheres. Any sudden shock or vibration to the mat will dislodge the spheres.

Many techniques were tried in order to retain the spheres on the glass fiber mat. This included either heating the mat before or after impregnation with the hollow glass spheres. The idea was to encapsulate the spheres in the thermoplastic binder of the mat. However, the low density of the spheres caused them to float on the binder and remain free. Another technique of coating the fiber mat after impregnation proved marginally successful. Here the idea was to coat both the spheres and the mat with a thermoplastic (e.g. polyamide) after impregnation to freeze the spheres in place. This resulted in a high fraction of polyamide on the mat.

While a method of successfully retaining glass spheres on glass fiber mat has not been found as yet, the above study has established that the aerosolization technique can be used to uniformly deposit the spheres into the fiber mat. The uniform distribution of filler will enable the final part to have uniform mechanical properties with possible weight savings.

Table 7.1 Parameters and weights of typical impregnation run

Mass of bed, gms	=	125
Relative amplitude (setting on amplifier)	=	4
Frequency, Hz	=	15
Initial mat weight, gms	=	45.77
Impregnation time, min	=	5
Impregnated mat weight, gms	=	50.1
Pick-up, weight %	=	9.46

**Figure 7.5** SEM photograph of hollow glass sphere on glass fiber

In addition the study has also demonstrated that the powder prepreg system can be adapted to other fiber-matrix systems. The requirement is that aerosolization of the powder should be possible and that the powder should adhere to the fiber. If these requirements are met, commercially attractive fiber-matrix systems could be used in the prepregging process.

Chapter 8

CONCLUSIONS

A number of conclusions can be drawn from the study presented in this thesis specific to polyamide powder and carbon fiber :

(1) The powder prepreg process is sensitive to charge to mass ratio variations. The smaller size particles ($\sim 5 \mu\text{m}$) exhibit extensive agglomeration and do not work well in the process. Their large charge to mass ratio causes large fluctuations in the operating curve for the process. Larger particle sizes result in a reduction of particle pick-up due to their poor aerosolization characteristics owing to their weight. Thus an optimum size range exists for the system.

In order to achieve a desired volume fraction of prepreg tape from the system with any given particle size within this range, it is necessary to determine the operating curve for the particular conditions (e.g., speed, fiber/matrix system, melt temperature, etc.). Once the operating curve is obtained, the volume fraction can be dialed in with only 2-3% error. The variation within each run depends on the length of the run and is within 5% for one hour runs. The main reason for this variation is the lack of motion control on the fiber tow.

(2) Under the conditions selected for this study, the consolidation process does not seem to be affected by particle size to the same extent as volume fraction. For the three size ranges that were used in this investigation the consolidation curves are almost the same.

(3) A number of flaws were found to exist in the present system. Some of these were eliminated during the course of this study. The buzzer mechanism has reduced the caking of the aerosolizer wall to a significant extent. Though many techniques have been tried to break up agglomeration, none were completely successful but the size of the agglomerates has been reduced to some degree. Problems with line speed control exist and some recommendations have been made.

(4) New applications were explored for the process. A simple technique for RTM preform manufacture has been developed. This preform shows good structural integrity and has good porosity. It is envisaged that this type of preform manufacture would eliminate porosity reduction due to shifting of the reinforcement during liquid molding.

(5) A new area of filler impregnation has been explored. This utilizes hollow glass spheres and a random glass fiber mat. A new aerosolizer capable of operating with the glass mats was constructed. Operating conditions for this new aerosolizer were determined. It has thus been demonstrated that the process can be adapted to other fiber-matrix systems.

(6) A simple model for the spreader has been developed. The approach used is semi-empirical. The model identifies the relationship between the important factors in the operation of the spreader.

The results of this investigation are by no means complete. A number of areas of the process are still not well understood. As a result of this study, some **recommendations for future work** can be made. These are listed below :

- Line speed control of the fiber tow needs to be improved. A new control strategy must be used. One viable technique has been described in Section 4.1.
- The problem of agglomeration of smaller particle size must be investigated and better methods to break up or reduce agglomeration must be developed.
- Other fiber-matrix systems must be investigated in order to make the process commercially attractive.
- The effect of particle size on processing time has not been established. A probable experimental program has been outlined in Section 6.2.
- A scaled-up system operating at higher speeds would make the process economically feasible.
- Data on the spreading process is not complete and experimentation with scaled-up units is necessary in order to develop a quantitative model for the unit operation.
- Finally, the powder prepreg process has many variables that need to be controlled to achieve optimum quality of the composite prepreg tape. The effects of all the variables is not entirely known. Further experimentation towards understanding the fundamental principles and operation need to be accomplished.

APPENDIX

APPENDIX

The estimation of sintering time for different particle sizes of polyamide is necessary in order to determine the operating temperature and residence time of the sintering oven. A viscosity model developed by Iyer [11] was used to relate the viscosity to the temperature. This is given by

$$\mu = a_T \mu_i \left[\frac{T}{T_o} \right]$$

$$\begin{aligned} \text{where } \log(a_T) &= 2.664031(1000/T) - 5.680173 & (13) \\ \log(\tau_r) &= 0.9813163 \log(\gamma) + 2.702483 \\ \mu_T &= \tau_r / \gamma \\ T_o &= \text{reference temperature} = 197.3 \text{ } ^\circ\text{C} \end{aligned}$$

This model was substituted into Frenkel's model for estimating sintering times [10]. The model predicts sintering times based on viscosity and particle size and is given by

$$\frac{x^2}{r} = \frac{3}{2} \left[\frac{\gamma}{\mu} \right] t \quad (14)$$

where

x = radius of inter-particle bridge

r = radius of particle

γ = polymer melt surface tension

μ = polymer viscosity (function of temperature)

t = sintering time

The variation is calculated using a computer program written in BASIC. A listing of this program code follows.

```

10 REM : PROGRAM TO CALCULATE SINTERING TIME AS A FUNCTION
20 REM : OF TEMPERATURE AND PARTICLE SIZE
30 OPEN "C:VISC.RES" FOR OUTPUT AS #1
40 FOR PS=5 TO 50 STEP 5
50 FOR TEMP=150 TO 230 STEP 10
60 AT=10^(2664/(TEMP+273)-5.68)
70 MU=AT*527.23*(273+TEMP)/(273+197.3)
80 TIME=2*(PS*.000001/2)*MU*.1/(3*30*.00001*100)
90 PRINT PS,TEMP,TIME
95 PRINT #1,"PS", "TEMP", "TIME"
100 PRINT #1,PS,TEMP,TIME
110 NEXT TEMP
120 NEXT PS
130 END

```

The results are shown graphically in Figure 3.4.

BIBLIOGRAPHY

BIBLIOGRAPHY

- [1] Rudin, A., *The Elements of Polymer Science and Engineering*, Academic Press, Inc., 1982.
- [2] Carlsson, L. A. (editor), *Thermoplastic Composite Materials*, Elsevier Science Publishing Company, 1991.
- [3] Iyer, S. R., Drzal, L. T., "Dry Powder Processing of Thermoplastic Composites", *Fifth Technical Conference [Proc]*, p 259-266, American Society of Composites, 1990.
- [4] Iyer, S. R., "Continuous Processing of Unidirectional Prepreg", *Ph.D. Dissertation*, Michigan State University, 1990.
- [5] Iyer, S. R., Drzal, L. T., "Method and System for Spreading a Tow of Fibers", *U.S. Patent No. 5,042,111*, 1991.
- [6] Iyer, S. R., Drzal, L. T. and Jayaraman, K., "Method for Fiber Coating with Particles", *U.S. Patent Application*, Feb 1990.
- [7] Seborg, D. E., Edgar, T. F. and Mellichamp, D. A., *Process Dynamics and Control*, John Wiley and Sons, 1989.
- [8] Waterbury, M. C., Drzal, L. T., "Determination of Fiber Volume Fractions by Optical Numeric Volume Fraction Analysis", *J. Reinforced Plastics and Composites*, 8, p 627-636, 1989.
- [9] DSC 910 manual, DuPont Co.
- [10] Frenkel, J., *J. Physics U.S.S.R.*, 9, 385, 1945.
- [11] Iyer, S. R., "Continuous Processing of Unidirectional Prepreg", *Ph.D. Dissertation*, Michigan State University, p 79, 1990.
- [12] Iyer, S. R., "Continuous Processing of Unidirectional Prepreg", *Ph.D. Dissertation*, Michigan State University, p 89, 1990.
- [13] Reist, P. C., *Introduction to Aerosol Science*, MacMillan Pub. Co., 1984.

- [14] Geldart, D., "Types of Gas Fluidization", *Powder Technology*, 7, p 285-292, 1973.
- [15] Rietema, K., "Powders - What are they?", *Powder Technology*, 37, 5, 1984.
- [16] Visser, J., "Van der Waals and other Cohesive Forces affecting Powder Fluidization", *Powder Technology*, 58, p 1-10, 1989.
- [17] Grace, J. R., *Can. J. Chem. Engg.*, 64, p 353, 1986.
- [18] Glor, M., Electrostatic Hazards in Powder Handling, *John Wiley and Sons Inc.*, 1988.
- [19] Sheehan, D. P., Carillo, M. and Heidbrink, W., "Device for the Dispersal of Micrometer- and Submicrometer-sized Particles in Vacuum", *Rev. Sci. Instrum.*, " 61 (12), p 3871-3875, 1990.
- [20] RAM-S Manual, *M.I.E. Inc.*.
- [21] Perry, R. H., Green, D. W. (editors), *Perry's Chemical Engineers' Handbook*, Sixth Edition, *McGraw Hill Book Company*, 1984.
- [22] Fallstrom, K.-E., "Determining Material Properties in Anisotropic Plates using Rayleigh's Method, *Polymer Composites*, 12, 5, p 306-314, 1991.
- [23] Iyer, S. R., "Continuous Processing of Unidirectional Prepreg", *Ph.D. Dissertation*, Michigan State University, p 123, 1990.
- [24] Iyer, S. R., "Continuous Processing of Unidirectional Prepreg", *Ph.D. Dissertation*, Michigan State University, p 144-149, 1990.
- [25] Chawla, K. K., *Composite Materials Science and Engineering*, *Springer-Verlag*, 1987.
- [26] Iyer, S. R., "Continuous Processing of Unidirectional Prepreg", *Ph.D. Dissertation*, Michigan State University, p 162, 1990.
- [27] Lubin, G., *Handbook of Composites*, *Van Nostrand Reinhold*, 1982.
- [28] Narkis, M., Chen, E. J. H., "Unidirectional Hybrid Thermoplastic Composites Reinforced with Continuous Fiber and Glass Spheres", *SAMPE Journal*, 26, 3, p 11-15, 1990.

MICHIGAN STATE UNIV. LIBRARIES



31293010490930